Systematic Revision of the Genus *Charmus* Karsch, 1879 (Scorpiones: Buthidae), and Assessment of Its Phylogenetic Position Within Buthidae C. L. Koch, 1837 Using Ultraconserved Elements

Mihir Joshi [1,2], Shubhankar Deshpande [1], Sajiri Ukale [1,2], Gaurang Gowande [1,3], Julia Bilat [4], František Kovařík [5], Hélène Mottaz [4], František Šťáhlavský [5], Deshabhushan Bastawade [1], Lionel Monod [4] and Shauri Sulakhe [1,*]

1   Scorpion Systematics Laboratory (SSL), InSearch Environmental Solutions (IES), Flat no 1, Omkar Apartments, Near Shivaji Maharaj Statue, Sant Gangaram Road, Pune 411038, Maharashtra, India; mihirjoshi1604@gmail.com (M.J.); shubhankarsdeshpande11@gmail.com (S.D.); sajiriukale2003@gmail.com (S.U.); gaurang.gowande@gmail.com (G.G.); dbbastawade@gmail.com (D.B.)
2   Department of Biotechnology, Modern College of Arts, Science and Commerce, Shivajinagar, Pune 411005, Maharashtra, India
3   Annasaheb Kulkarni Department of Biodiversity, Abasaheb Garware College, Karve Road, Pune 411004, Maharashtra, India
4   Muséum D'histoire Naturelle, Route de Malagnou 1, 1208 Genève, Switzerland; julia.bilat@geneve.ch (J.B.); helene.mottaz@geneve.ch (H.M.); lionel.monod@geneve.ch (L.M.)
5   Department of Zoology, Charles University, Viničná 7, 128 44 Prague, Czech Republic; kovarik.scorpio@gmail.com (F.K.); frantisek.stahlavsky@natur.cuni.cz (F.Š.)
*   Correspondence: shauri.sulakhe@insearchenvs.org or shaurisulakhe@gmail.com

Abstract: India and Sri Lanka are known to exhibit high levels of biological diversity with many endemic taxa, such as the enigmatic scorpion genus *Charmus* Karsch, 1879. Members of this genus are rarely encountered in the field and are also known to be morphologically very similar, which impedes their systematic assessment. Our dedicated efforts towards sampling the members of the genus resulted in the collection of important material, which allowed us to carry out a thorough systematic revision of the genus using an integrated taxonomic approach. We propose several taxonomic changes based on the results of a detailed morphological study supported by molecular data. *Charmus indicus* Hirst, 1915 is synonymized with *Charmus laneus* Karsch, 1879, owing to the lack of morphological differences and low genetic divergence between the two taxa. We designate a neotype for *Charmus sinhagadensis* Tikader and Bastawade, 1983, and describe a new species from Sirumalai (Tamil Nadu, India). Moreover, we provide the first molecular phylogeny of *Charmus* based on Cytochrome c Oxidase subunit I (COI), 16S rRNA (16S) and 28S rRNA (28S) genes. The phylogenetic position of the genus within the family Buthidae C. L. Koch, 1837 is also tested using an independent genome-wide dataset (Ultraconserved Elements). Topological congruence and discrepancies between the phylogenies generated with Sanger sequences and the Ultraconserved Elements are commented on, and the reliability of these datasets when evaluating phylogenetic relationships at different hierarchical levels is further discussed.

Keywords: Indian sub-continent; endemism; biodiversity; new species; multi-locus phylogeny; genomics; Scorpiones; Buthidae; *Charmus*

1. Introduction

India and Sri Lanka are regarded as major biodiversity hotspots [1], harboring a rich array of endemic species and exhibiting interesting biogeographical patterns of species distribution. While these patterns have been recently studied for various herpetofaunal groups [2–4], they remain largely untested in arachnids, likely owing to the elusive nature and narrow distribution range of many of these arthropods. In addition to the difficulty of collecting them, the lack of morphological diagnostic characters has hampered the recognition of species based on alpha-taxonomy alone, and in such cases, molecular phylogenetics is the only tool that can then help with species differentiation [5–7]. The humicolous scorpions of the genus *Charmus* Karsch, 1879 (Figure 1), endemic to India and Sri Lanka, are one of these problematic taxa: difficult to identify to species level and seldom encountered in the field. The material is thereby very rare in museum collections. In our continuous efforts to resolve the systematics of Indian scorpions, we have recently carried out extensive fieldwork to collect additional *Charmus* specimens across Peninsular India. A thorough integrated systematic study of the material collected during these surveys allows us to thoroughly reassess the taxonomy of this enigmatic genus.

Figure 1. *Charmus sinhagadensis* Tikader & Bastawade, 1983 in vivo habitus at Sinhagad Fort, India. Scale bar: 5 mm. Photograph by Mihir Joshi.

1.1. Systematics of the Genus Charmus

The genus *Charmus* was first described based on the type species *Charmus laneus* Karsch, 1879 from Sri Lanka (formerly Ceylon) [8]. The species *Charmus indicus* Hirst, 1915 was described from Coimbatore (Tamil Nadu, India) based on a single immature specimen [9]. Reddy [10] subsequently redescribed *C. indicus* and documented its distribution in southern Peninsular India with the report of multiple new localities. However, none of the specimens examined in the scope of this redescription were collected from the designated type locality.

Subsequently, *Charmus sinhagadensis* Tikader & Bastawade, 1983 [11] was described from Sinhagad Fort (Pune, Maharashtra, India), making it the northernmost record of the genus. Lourenço [12] described *Charmus brignolii* Lourenço, 2000 from Puducherry (formerly Pondicherry, Tamil Nadu, India) and later *Charmus minor* Lourenço, 2002 [13] from Wilpattu National Park (Sri Lanka). Kovařík et al. [14] synonymized *C. minor* with the type species *C. laneus* Karsch, 1879 and described *Charmus saradieli* Kovarik et al., 2016 from the Central Province of the country, in a region that represents a transition area between dry and wet habitats.

Several taxonomic changes are proposed in the present study. Due to high morphological and molecular similarity, *C. indicus* is synonymized with *C. laneus*. Our investigations of the arachnological collections of the Zoological Survey of India (ZSI) also suggest that the holotype of *C. sinhagadensis* is lost, compelling us to designate a neotype following the recommendations of Article 75 of the International Code of Zoological Nomenclature (ICZN) [15]. Finally, a new species of *Charmus* is described from southern India.

1.2. Phylogenetic Analysis of the Genus Charmus

For a long time, morphological characteristics have served as the primary basis for species identification [16]. Nowadays, molecular phylogeny is used more often as a supplementary line of evidence for taxonomic amendments [17–19]. Interestingly, conflicts at supra-specific levels between modern molecular phylogenies and traditional morphology-based classifications have been repeatedly demonstrated not only in scorpions [20–22] but also in other arthropod groups [23–27]. Moreover, it appears that different molecular datasets are not informative at the same taxonomic scales [28]. The standard Sanger genetic markers used in phylogenetic and phylogeographic studies are usually adequate for resolving relationships at the species and population levels, but not at the generic level or above [29]. On the other hand, genome-wide datasets provide more signals for phylogenetic inference at higher taxonomic levels [30–35] but may perform poorly when assessing shallower nodes. For instance, phylogenetic information at shallow time depths, e.g., intraspecific levels, recovered by UCE loci depends entirely on the length of the flanking regions captured in the process [36]. Based on these considerations, the interspecific relationships within the genus *Charmus* as well as the position of the genus within the family Buthidae C. L. Koch, 1837 was assessed by phylogenetic analyses of two independent molecular datasets, one composed of Sanger-generated sequences, and one composed of UCE loci that are either newly generated or harvested from available transcriptomic data. Topological congruence and/or discrepancy between the two phylogenies obtained were then assessed. The reliability of the different datasets to reconstruct phylogenetic relationships at different hierarchical taxonomic levels was then discussed based on this comparison.

2. Materials and Methods

2.1. Specimen Collection and Morphological Data

Fieldwork was carried out in the Northern Western Ghats and Southern India, especially in the coastal region and in parts of Eastern Ghats. Scorpions were located with the help of ultraviolet light (uvBeast V3 385–395 nm UV Torch) at night and collected using forceps. Specimens were euthanized and preserved in absolute ethanol and later transferred to vials containing 70% ethanol for long-term preservation. Photographs of the preserved specimens were taken using a D500 (Nikon Corporation, Tokyo, Japan), 105 mm F2.8 microlens and Nikkor 60 mm f/2.8 microlens with a MF12 flash kit (Godox Photo Equipment Co. Ltd., Shenzhen, China). Specimens were examined and morphological measurements were recorded using a EZ4HD microscope (Leica Camera AG, Wetzlar, Germany) with the Leica application suite.

Trichobothrial terminology follows Vachon [37]; metasoma carination follows Francke [38]; pedipalp carination, chela dentition, and leg terminology follow González Santillán and Prendini [39]; morphological terminology follows Hjelle [40]; lateral ocelli terminology follows Loria and Prendini [41]. Surface morphology was examined and photographed under UV light after Volschenk [42]. Measurements following Stahnke [43] were taken (in mm) for 34 morphological characters, to the nearest 0.1 mm.

2.2. Repository

Specimens collected during this study are deposited in the collections of the Bombay Natural History Society (BNHS, Mumbai, Maharashtra, India) and of InSearch Environmental Solutions (IES, Pune, Maharashtra, India). Other specimens are housed in the British Museum of Natural History (BMNH, London, UK), Muséum National d'Histoire Naturelle (MNHN, Paris, France) and the Museum für Naturkunde der Humboldt Universität (ZMB, Berlin, Germany).

2.3. Taxon Sampling

Data for the Sanger sequence-based phylogeny (Table S4) are as follows. The ingroup includes the four species of *Charmus* known from the Indian subcontinent, i.e., *C. brignolii*, *C. laneus*, *C. saradieli*, *C. sinhagadensis* and the newly described *Charmus dakshini* sp. nov. Each of the five species is represented by more than one sample (2–4) except *C. saradieli*. Outgroup data were sourced from Štundlová, et al. [22] and are composed of 48 species belonging to 48 genera of the family Buthidae and two species of the genus *Protoiurus* Soleglad, Fet, Kovařík & Yağmur, 2012 (Iuridae Thorell, 1876).

Data for the UCE phylogeny (Table S5) are as follows. The ingroup is composed of three species of *Charmus,* i.e., *C. brignolii*, *C. sinhagadensis* and *C. dakshini* sp. nov. Each of the three species is represented by two distinct populations. The outgroups include sequences of two *Buthoscorpio* Werner, 1936, generated in the course of the present work, as well as additional UCE [44,45] and transcriptomic data [20] available to the scientific community through the Sequence Read Archive (SRA) accessible on the NCBI portal. The data downloaded from NCBI consist of a total of 35 species belonging to 22 genera of the family Buthidae, one species of the genus *Chaerilus,* two species belonging to two genera of the family Pseudochatidae Gromov, 1998 and one species of the genus *Iurus* (Iuridae Thorell, 1876).

2.4. Sanger Sequencing: DNA Extraction, Amplification and Sequencing

DNA extraction, amplification and sequencing protocols from Sulakhe et al. [46] were followed to generate data on the Indian *Charmus* species. A 550–600 base pair (bp) fragment of the cytochrome c oxidase subunit I (COI), a 450–500 bp fragment of 16S rRNA (16S) mitochondrial genes and a 700–750 bp fragment of 28S nuclear gene were amplified by polymerase chain reaction (PCR) using the primers (Table S7) as in previous studies [5,47–50]. All newly generated sequences were deposited at GenBank® [51].

2.5. Sequence Alignment of the Sanger Sequenced Data

Generated sequences were cleaned manually in MEGA v.7 [52], using chromatograms visualized in Chromas v.2.6.5 (Technelysium PTY. Ltd., South Brisbane, QLD, Australia). Cleaned sequences were aligned using MUSCLE [53], implemented in MEGA v.7 with default parameters. Separate alignments were built for COI, 16S, and 28S. The final COI alignment contained 62 sequences (each 525 bp long), the 16S alignment contained 55 sequences (each 359 bp long), and the 28S alignment contained 49 sequences (each 733 bp long). The COI, 16S and 28S datasets were concatenated, and the resultant 1617 bp long alignment was used for molecular phylogenetic analyses.

2.6. Genetic Divergence (p-Distance) of the Sanger Sequenced Data

Uncorrected *p*-distances were calculated separately for COI, 16S, and 28S in MEGA v.7. Missing data were partially deleted, and the site cut-off was set at 95%.

2.7. Molecular Phylogenetic Analysis of the Sanger Sequenced Data

Maximum Likelihood (ML) methods were implemented for phylogenetic analyses. The COI region was partitioned by codon position, whereas the non-coding 16S and 28S regions were not partitioned. Analyses were performed using the web implementation of IQ-TREE [54] and RAxML GUI [55]. For IQ-TREE, models of sequence evolution were determined using ModelFinder [56] which were as follows: TPM2 + FG4 for COI position 1, TIM3 + F + I + G4 for COI positions 2 and 3; TVM + F + I + G4 for 16S and TIM3 + F + I + G4 for 28S. One thousand ultrafast bootstraps (UFBoot) [57], were used to test nodal support [58]. The best substitution model for RAxML was determined using PartitionFinder v.1.1.1 [59]. Model search was performed with a greedy search algorithm [60], and models were selected using the Akaike Information Criterion (AIC). The dataset was partitioned, and the analysis was run using the GTR + I + G evolutionary model using 1000 bootstrap pseudo-replicates.

2.8. DNA Extractions and Shotgun Library Preparation

Total genomic DNA from the representatives of *Charmus* and *Buthoscorpio* was extracted from leg muscle tissues separately for UCE analyses using QIAamp DNA micro kits following the manufacturer's protocol. The DNA length and quality were quantified using a Fragment Analyzer (FA). Samples with 50 to 600 bp DNA fragments were considered optimal for library preparation. Samples with longer DNA fragments were sheared using NEBNext® dsDNA Fragmentase® (New England Biolabs, Ipswitch, MA, USA) to reduce their size. The modified version of the protocols used by Suchan et al. [61], based upon Meyer et al. [62], were followed for the shotgun library preparation. The purified DNA was first phosphorylated using T4 polynucleotide kinase and T4 ligase buffer. The double-stranded DNA was further denatured at 95 °C for 5 min and then immediately chilled in water and ice mix. The guanine tail was added using the Terminal Transferase (TDT) reaction mix. A complementary strand was synthesized with Klenow Fragment and poly-C oligonucleotide. The blunt-end reaction was performed using T4 DNA polymerase and barcode adapters were ligated to the phosphorylated end opposite to the poly-C end using T4 DNA ligase. The adapter sequences were filled in using the *Bst* DNA Polymerase, and two PCR replicates were run using Phusion U Hot Start DNA Polymerase (Thermo Fisher Scientific, Waltham, MA, USA) and indexed PCR primers. The two PCR replicates were put together, and library concentrations were quantified in a Quant-iT PicoGreenR dsDNA reagent (Invitrogen, Thermo Fisher Scientific, Waltham, MA, USA) on a Hidex Sense Microplate Reader (Hidex Oy, Turku, Finland). For the capture, 12 equimolar pools of 8 libraries each were prepared and concentrated with an IR Micro-Cenvac NB-503CIR Vacuum Concentrator (N-Biotek, Bucheon, Republic of Korea).

2.9. Hybridization Capture and Sequencing of UCEs

Hybridization capture for the enrichment of shotgun libraries followed the myBaits protocol (Arbor Biosciences, Ann Arbor, MI, USA) using the UCE Arachnida 1.1Kv1 probe set [44,63]. The adaptor blockers and standard myBaits blockers were annealed to the library pools, and the resulting strands were hybridized to the arachnid probes. Two successive sets of UCE captures were performed at two different temperatures, one at 55 °C and the second at 65 °C. The second capture was performed at a higher temperature as it improved

the stringency of the reaction. Library sequencing paired-end runs were performed on Illumina HiSeq X (Macrogen, Seoul, Republic of Korea) to produce 150 bp-long reads.

2.10. Data Processing and PHYLUCE Pipeline

The adapters were removed from the sequenced raw reads using a custom script. The reads were assembled using Trinity v. r2013-02-25 [64] and SPADES [65]. Contigs resulting from both assemblies were combined using a custom protocol. This allowed an increase in the number of recovered UCEs. The combined Trinity/Spades contigs were then processed using the PHYLUCE pipeline [66]. UCE loci were aligned using MAFFT [67] and trimmed with Gblocks [68,69] as implemented in the PHYLUCE pipeline. UCE loci were extracted from transcriptomic data using the PHYLUCE pipeline. The resulting individual UCE alignments were manually edited, and erroneous base pairs were treated as missing data. 87–918 UCES and 249–877 UCEs from transcriptomic data were retrieved. Each of the 1030 alignments was manually verified and potential alignment errors were corrected. The number of UCEs retrieved after sanitation of the alignments is indicated in Table S5. Four different occupancy matrices (20%, 50%, 70% and 80%) were generated with the sanitated alignments for phylogenetic analysis.

2.11. Phylogenetic Analyses of the Generated UCE Matrices

Maximum Likelihood analyses were performed with each of the assembled matrices using RAxML HPC v8.0 [70] and IQ-TREE [54] for each data matrix. For the RAxML analyses, the GTRCAT substitution model was implemented and the autoMRE option was selected, whereas, for the IQ-TREE analyses, the best-fit substitution model was automatically selected using TESTNEWMERGE as GTR + F + I + G4. One thousand ultrafast bootstrap replicates (UFBoot) [57] were used to test the nodal support [58].

3. Systematics

Family Buthidae C. L. Koch, 1837

Genus *Charmus* Karsch, 1879

Figures 2–20, Table 1, Table 2, Table 3, Table 4, Table 5, Table 6 and Table S1–S6

Charmus Karsch, 1879: 104; Kraepelin, 1899: 39; Pocock, 1900: 31–32; Kraepelin, 1913: 131; Vachon, 1982: 79, 81; Tikader & Bastawade, 1983: 140–152; Sissom, 1990: 101; Kovařík, 1998: 120; Lourenço, 2000: 295; Kovařík, Soleglad & Fet, 2007: 201; Kovařík, 2009: 31. *Heterocharmus* Pocock, 1892: 46–47, type species by monotypy *Heterocharmus cinctipes* Pocock, 1892 (=*Charmus laneus* Karsch, 1879) (syn. by Kraepelin, 1899: 39; Pocock, 1900: 31) Kovařík et al., 2016: 17–29, figs. 12, 41–43, 47–119, 194, 423–426, 548, Tables 1 and 2.

Type species: *Charmus laneus* Karsch, 1879

Diagnosis: Small scorpions, adult size 12 mm (male)–23.5 mm (female). Sternum type 1, subpentagonal, roughly as wide as long, exhibiting horizontal compression. Pedipalps trichobothrial pattern Aα; femur trichobothrium d_2 located dorsally, patella d_3 dorsal of dorsomedian carina; chela with 3 *Eb* trichobothria on manus. Movable finger of pedipalp longer than manus. Pectines with or without fulcra. Dentate margin of pedipalp chela movable finger with distinct granules divided into 8–9 linear rows, apical rows of 4–6 granules, and 3 terminal granules. Cheliceral fixed finger armed with two denticles on ventral surface. Tergites I–VI granular, with one clearly visible carina. Carapace granular without carinae, anterior edge with epistome present medially. Ventral surface of metasomal segments IV–V without developed carinae. Telson vesicle punctate, without subaculear tooth. Pedipalps, metasoma and telson densely hirsute. Legs III and IV with well-developed long tibial spurs, first and second tarsomeres with ventral setae.

Distribution: India and Sri Lanka.

3.1. Charmus laneus Karsch, 1879

Figures 2–4, 10 and 15–20, Table 1

Holotype (not examined): Ceylon (=Sri Lanka), leg. Hoffmeister, 1 ♀(ZMHB No. 3051). Other material: India, Tamil Nadu, Coimbatore, 388 m, 29th June 2023, leg. Shauri Sulakhe, Shubhankar Deshpande, Mihir Joshi, 2 ♂(IES 631, IES 633), 2 ♀(IES 628, IES 629), one juvenile (IES 632).

Synonym:

Charmus indicus Hirst, 1915 syn. nov.

Holotype (not examined): leg. T. Bainbrigge Fletcher, ♂(BMNH Regd. No. 1915.10.16.1). Other material (not examined): Udaygiri Fort, leg. Dr. A.P. Mathew, 1 ♂(MNHN, Paris, R. S. 3017); Tirupati, Andhra Pradesh, 3 ♂, 1 ♀(MNHN, Paris, R. S. 4407).

Description (♂, IES 631, measurements in Table 1):

Coloration (Figure 2A,B): body dorsal surface entirely black with dark brown stripes on the median portion of mesosoma; legs dark brown with alternate yellow and black stripes with tarsomere dark brown; metasoma almost black; pedipalp fingers dark brown. Ventral surface yellow except last mesosomal sternite black. Basal segments of chelicerae dark brown with black reticulation ending anteriorly into black transverse patch. Fingers of chelicerae blackish brown with the tip of the fingers black. Telson dark brown in color.

Table 1. Measurements and meristics of *Charmus laneus* Karsch, 1879 (in mm).

		IES-631 (♂)	IES-633 (♂)	IES-628 (♀)	IES-629 (♀)	IES-632
Carapace	L/W	2.08/1.81	1.71/1.55	1.99/2.02	2.03/1.9	2.12/1.94
Mesosoma	L	4.48	3.62	4.6	5.35	2.47
Tergite VII	L/W	0.95/1.99	0.83/1.58	0.95/1.73	1.91/1.62	0.55/1.28
Metasoma and telson	L	8.55	7.83	10.47	8.84	6.09
Segment I	L/W/D	0.97/1.48/1.23	0.93/1.3/1.1	1.32/1.53/1.27	0.87/1.5/1.25	0.76/0.89/0.76
Segment II	L/W/D	1.21/1.4/1.2	0.99/1.22/1.15	1.61/1.57/1.42	1.05/1.52/1.26	0.86/0.87/0.80
Segment III	L/W/D	1.34/1.44/1.21	1.15/1.28/1.21	1.85/1.54/1.42	1.25/1.52/1.39	0.93/0.96/0.82
Segment IV	L/W/D	1.51/1.48/1.18	1.35/1.29/1.24	2.12/1.54/1.42	1.59/1.52/1.36	1.06/0.95/0.85
Segment V	L/W/D	1.63/1.46/1.12	1.7/1.31/1.16	2.45/1.6/1.33	2.25/1.5/1.26	1.34/1.99/0.81
Telson	L/W/D	1.14/0.8/0.9	0.96/0.77/0.89	0.63/0.50/0.99	0.91/0.8/0.95	0.62/0.46/0.54
Pedipalp	L	6.63	5.29	6.78	6.54	4.03
Femur	L/W	1.72/0.51	1.35/0.48	1.65/0.54	1.72/0.55	0.98/0.39
Patella	L/W	2.00/0.78	1.62/0.69	2.15/0.79	1.97/0.75	1.26/0.46
Chela	L	2.91	2.32	2.98	2.85	1.79
Manus	W/D	0.6/0.6	0.48/0.54	0.63/0.66	0.66/0.64	0.37/0.39
Movable finger	L	1.65	1.75	1.91	2.04	1.08
Pectine	L/W	1.72/0.43	1.60/0.39	1.74/0.47	1.71/0.42	0.99/0.26
Genital Operculum	L/W	0.43/0.62	0.28/0.47	0.38/0.72	0.42/0.68	0.22/0.36
Total	L	15.11	13.16	17.06	16.22	10.68
Pectinal teeth count	PTC	17/16	15/16	16/17	16/17	17/17

Carapace (Figures 3A and 15A): surface with mixed and dense granulation. Carapace without carinae. Median supra-ocular area with few sparse granules. Interocular area coarsely and densely granular. A pair of median eyes situated anteriorly in the ratio 1:1.6 (ratio of median eyes to anterior margin and median eyes to posterior margin). Antero-lateral ocular tubercle granular with type 3A ocelli. Three well-developed lateral ocelli

with first and third ocelli smaller than the second ocelli. Longitudinal furrow shallow anteriorly and deep posteriorly. Anterior margin finely crenulated in the median portion and straight throughout. Lateral margins weakly crenulated below lateral ocelli. Posterior margin almost entirely smooth.

Chelicerae: characteristic of the family Buthidae. Basal segments and movable fingers with tuft of short and firm setae on ventral surfaces. Dorsal surfaces smooth.

Pedipalp (Figures 2A,B and 3C–I): femur with five carinae (prodorsal, retrodorsal, promedian, proventral and retroventral). All carinae crenulated. Intercarinal surfaces with mixed and sparse granulation except ventral surface smooth with a few fine granules on proximal portions. Patella almost smooth without developed carinae except promedian carina moderately developed with 7 spinoid granules. Intercarinal surfaces almost smooth. Manus smooth without carinae. Fixed fingers acarinate. Movable and fixed fingers with eight oblique rows of granules, each row (except most proximal) with one internal accessory granule. Trichobothrial pattern of type Aα, typical for the genus (chela dorsal 2, chela rerolateral 10, chela ventral 2, patella dorsal 6, patella retrolateral 7, femur dorsal 7 and femur prolateral 4).

Figure 2. *Charmus laneus* Karsch, 1879; adult ♂ (IES-631); (**A**) Dorsal view (**B**) Ventral view. Scale bar: 5 mm. Remark: Metasomal segments II-IV are broken and this individual was photographed due to unavailability of additional intact adult male specimens.

Legs (Figure 2A,B): femur and patellae carinated. Tibiae III and IV carinated, with long tibial spurs. All legs with a pair of pedal spurs. Tarsomere covered with long delicate setae arranged in parallel rows on ventral side. Tarsomere I (basitarsus) with a tuft of short, stout golden setae on ventral side. Tarsomere II (telotarsus) with a small bulge situated

laterally on the proximal portion. Tarsomere II compressed laterally and ventrally with paired row of short, pointed, anteriorly directed, closely placed setae. Tarsomere II with a single row of granular carina on the ventral surface.

Genital operculum (Figure 3B): wider than long, elliptical, separated with a pair of short male genital papillae.

Pectines (Figures 3B and 16A): Basal piece moderately notched on anterior median margin, lateral areas of posterior margin curved anteriorly. Marginal lamella of 3/3 digits and median lamella of 7/7 digits, outer margin armed with a row of stout short golden setae and few setae on surface. Fulcra 16/16, very small, roughly triangular, each armed with few short golden setae, placed in between adjacent pectinal teeth. Teeth 16/16, strong and stout.

Mesosoma (Figure 2A,B): tergites I–VI with mixed granulation with median carina moderately developed throughout except vestigial on the first segment. Posterior margin and lateral margins almost smooth. Tergite VII strongly and densely granular, narrowed posteriorly, with two pairs of lateral granular carinae. Sternites III–VI smooth, each with a pair of spiracles. Sternite VII with two pairs of weakly developed granular carinae present on two-thirds posterior portion. Intercarinal surfaces strongly and sparsely granular.
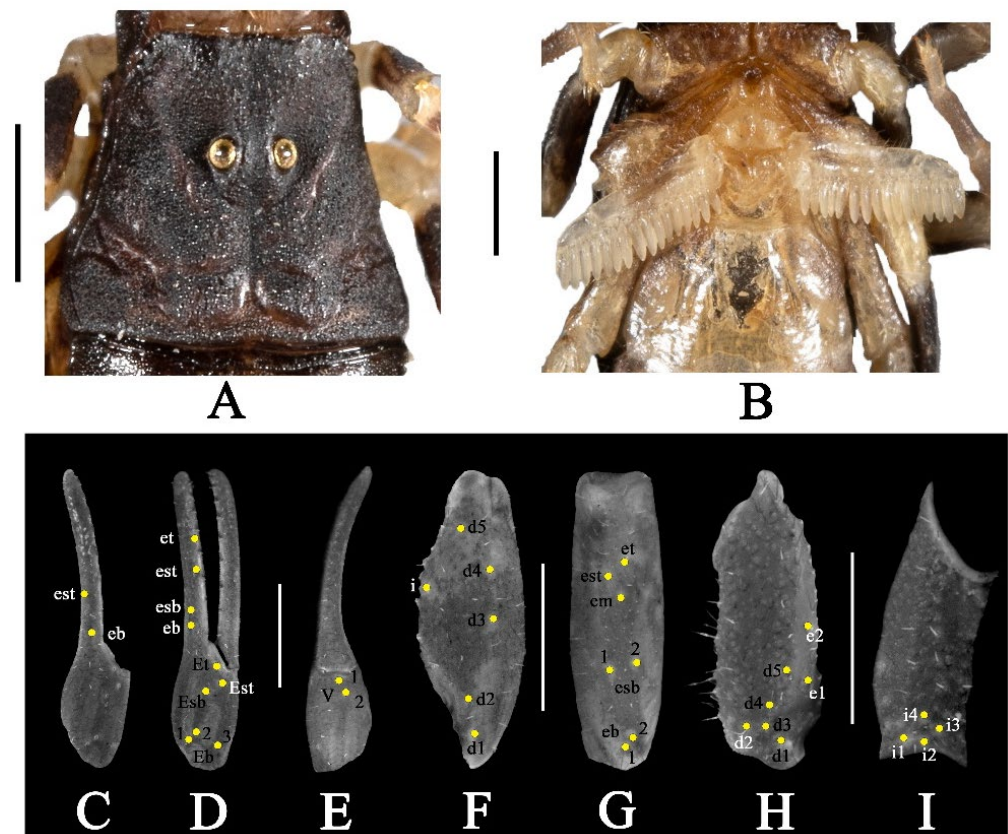

Figure 3. *Charmus laneus* Karsch, 1879; adult ♂ (IES-631); (**A**) carapace, white light (**B**) sternopectinal area (**C**–**I**) trichobothrial pattern on (**C**–**E**) Chela, (**C**) dorsal view. (**D**) External view, (**E**) ventral view; (**F**,**G**) patella, (**F**) dorsal view, (**G**) external view; (**H**,**I**) femur, (**H**) dorsal view, (**I**) internal view. Scale bars: 1 mm.

Metasoma (Figures 2A,B, 17A, 18A, 19A and 20A): all segments longer than wide. All segments punctate and strongly hairy with few long and few short setae. Segment I with four pairs of granular carinae (dorsal lateral, lateral supramedian, ventral lateral and ventral submedian). Segment II with five pairs of carinae (dorsal lateral, lateral supramedian, lateral inframedian, ventral lateral and ventral submedian). Segment III

with three pairs of carinae (dorsal lateral, ventral lateral and ventral submedian). Dorsal lateral carinae of segment I–III ending posteriorly into a short tubercle. Ventral submedian carina on segments I–III strongly developed. Segment IV and V heavily punctate and hairy. Segment IV with a pair of moderately developed dorsal lateral carina present on the anterior and posterior portions. Segment V with a pair of moderately developed dorsal lateral carina present on the anterior portion. Anterior ventral portion of Segment IV and posterior ventral portion of segment V with few scattered granules. Intercarinal surfaces of segments I–III strongly and densely granular except surface between dorsal lateral carinae and ventral lateral carinae of segment III almost smooth. Anal rim with two margins, lower margin moderately crenulated and upper margin weakly crenulated.

Telson (Figures 2A,B, 17A, 18A, 19A and 20A): telson punctate and hairy. Stout and globular without carinae. A depression present on dorsal lateral surface of vesicle. Proximal portion of vesicle with a pair of weakly developed nodule. Aculeus elongated and strongly curved.

Distribution, habitat and ecology (Figure 4): the specimens of *C. laneus* were collected from low-lying open fields surrounding the city of Coimbatore, Tamil Nadu, India. The individuals were found active at night, hiding under short grasses and were seen to be sympatric with other buthids such as *Buthoscorpio* sp. and *Hottentota* sp.

Figure 4. Scrub forests surrounding Coimbatore, India, from where the specimens of *Charmus laneus* Karsch, 1879 were collected. Photo by Gopan Madathil.

Remarks:

The species *Charmus indicus* Hirst, 1915 syn. nov. was collected and described from Coimbatore (Tamil Nadu) as the first occurrence of the genus from India. This description was incomplete and based on an immature specimen of unknown sex. Subsequently, Reddy [9] redescribed *C. indicus* based on adult specimens of both sexes from new localities (Tirupati, Andhra Pradesh; Udayagiri Fort and Puducherry, Tamil Nadu). However, no specimens from the type locality were present in his large sampling. Hirst [8] distinguished *C.indicus* from *C. laneus* based on the following diagnostic characteristics: (1) shortness and stoutness of tail, (2) presence of punctures (instead of granules) on the sides of the metasomal segment III (3) numerous punctures on metasomal segments IV and V

and (4) absence of granules from the ventral surfaces of metasomal segments IV and V (Figures 17A, 18A and 19A). However, the morphology of the specimens collected during our own field work from the original type locality of *C. indicus* as well as the morphology of *C. laneus* specimens from Sri Lanka photographed by Kovarik et al. [13] (Figures 71–73, p. 19) are congruent with all the abovementioned diagnostic characters. This strongly suggest that *Charmus* sampled from Coimbatore are not *C. indicus* but rather *C. laneus*. These specimens show the following combination of characters that are typical of *C. laneus*: (1) surface of carapace with mixed and dense granulation; (2) tergites I–VI with mixed granulation; (3) strongly developed ventral submedian carina on metasomal segments I-III. Therefore, according to Article 23 of the ICZN, we hereby propose to transfer *C. indicus* under the junior synonymy of *C. laneus*.

3.2. Charmus sinhagadensis Tikader and Bastawade, 1983

Figures 5–7, 10 and 15–20, Table 2

Holotype (considered lost): India, Maharashtra, Pune City, Sinhagad Fort, leg. D. B. Bastawade, ♀(ZSI No. 5079/18). Paratype (considered lost): same data as holotype, ♀(ZSI No. 5080/18). Neotype (designated here): India, Maharashtra, Pune City, Sinhagad Fort, 18.3663° N, 73.7559° E, 1315 m a.s.l., 5 May 2023, leg. Mihir Joshi, Aarya Gramopadhye, Aditya Soman, Akash Joshi, ♂(BNHS SC 403). Other material examined: Same data as neotype, 2 ♂(IES 587, IES 602). India, Maharashtra, Kolhapur District, Amba Ghat, 17.00° N, 73.777° E, 455 m a.s.l., 21 October 2019, leg. Makarand Ketkar, Akshay Marathe, ♂(IES-405); India, Maharashtra State, Pune District, Bhimashankar Wildlife Sanctuary, 19.0728° N, 73.5565° E, 997 m a.s.l., 10 December 2022, leg. Makarand Ketkar, Akshay Marathe, ♂(IES 561).

Table 2. Measurements and meristics of *Charmus sinhagadensis* Tikader and Bastawade, 1983 (in mm).

		BNHS SC 403 (♂) (Neotype)	IES-602(♂)	IES-587 (♂)
Carapace	L/W	2.27/2.28	1.8/1.56	1.82/1.58
Mesosoma	L	4.78	3.32	3.23
Tergite VII	L/W	1.21/2.52	0.94/1.63	0.86/1.62
Metasoma and telson	L	10.62	8.53	8.48
Segment I	L/W/D	0.88/1.50/1.26	0.96/1.11/1.05	0.94/1.1/1.13
Segment II	L/W/D	1.29/1.31/1.27	1.12/1.11/1.05	1.15/1.1/1.14
Segment III	L/W/D	1.50/1.35/1.38	1.39/1.11/1.09	1.26/1.11/1.13
Segment IV	L/W/D	2.18/1.36/1.31	1.45/1.14/1.1	1.52/1.1/1.12
Segment V	L/W/D	2.56/1.36/1.26	1.87/1.15/1.08	1.78/1.1/1.07
Telson	L/W/D	1.24/0.84/1.05	0.93/0.81/0.73	1.17/0.76/0.93
Pedipalp	L	9.08	5.95	6.14
Femur	L/W	2.19/0.67	1.5/0.48	1.57/0.46
Patella	L/W	2.81/0.98	1.83/0.63	1.83/0.66
Chela	L	4.08	2.62	2.74
Manus	W/D	0.86/0.84	0.54/0.53	0.54/0.55
Movable finger	L	2.81	1.78	2.02
Pectine	L/W	2.04/0.52	1.54/0.37	1.6/0.36
Genital Operculum	L/W	0.43/0.96	0.35/0.56	0.37/0.55
Total	L	17.67	13.65	13.53
Pectinal teeth count	PTC	14/14	15/15	15/15

Description (♂neotype, BNHS SC 403, measurements in Table 2):

Coloration (Figure 5A,B): body dorsal surface entirely dark brownish to blackish, except tergites with a brick red median longitudinal patch; legs dark brown with tarsomere yellowish brown; metasoma dark brownish to blackish; pedipalp fingers dark yellow. Ventral surface light yellow except last mesosomal sternite light brown. Basal segments of chelicerae yellow with black reticulation ending anteriorly into black transverse patch. Fingers of chelicerae blackish brown with tip of the fingers brown. Telson dark reddish brown in color.

Figure 5. *Charmus sinhagadensis* Tikader & Bastawade, 1983; neotype, adult ♂(BNHS SC 403); (**A**) Dorsal view (**B**) Ventral view. Scale bar: 5 mm.

Carapace (Figures 6A and 15B): surface finely and densely granular. Carapace without carinae. Median supra-ocular area smooth with few sparse granules. Interocular area finely and sparsely granular. A pair of median eyes situated anteriorly in the ratio 1:2.1 (ratio of median eyes to anterior margin and median eyes to posterior margin). Antero-lateral ocular tubercle granular with type 3A ocelli. Three well developed lateral ocelli, all three ocelli of same size. Longitudinal furrow shallow anteriorly and deep posteriorly. Anterior margin smooth throughout and slightly curved. Lateral margins smooth below lateral ocelli. Posterior margin almost entirely smooth.

Chelicerae: characteristic of the family Buthidae. Basal segments and movable fingers with tuft of short and firm setae on ventral surfaces. Dorsal surfaces smooth.

Pedipalp (Figure 5A,B, Figure 6C–I and Figure 10B): femur with five carinae (prodorsal, retrodorsal, promedian, proventral and retroventral). All carinae crenulated. Intercarinal surfaces with mixed and sparse granulation except ventral surface smooth with a few fine granules on proximal portions. Patella almost smooth without developed carinae except promedian carina weakly developed with 7 spinoid granules. Intercarinal surfaces almost smooth. Manus smooth without carinae. Fixed fingers acarinate. Movable and fixed fingers with eight oblique rows of granules, each row (except most proximal) with one internal accessory granule. Trichobothrial pattern of type Aα, typical for the genus (chela dorsal 2, chela retrolateral 10, chela ventral 2, patella dorsal 6, patella retrolateral 7, femur dorsal 7 and femur prolateral 4).
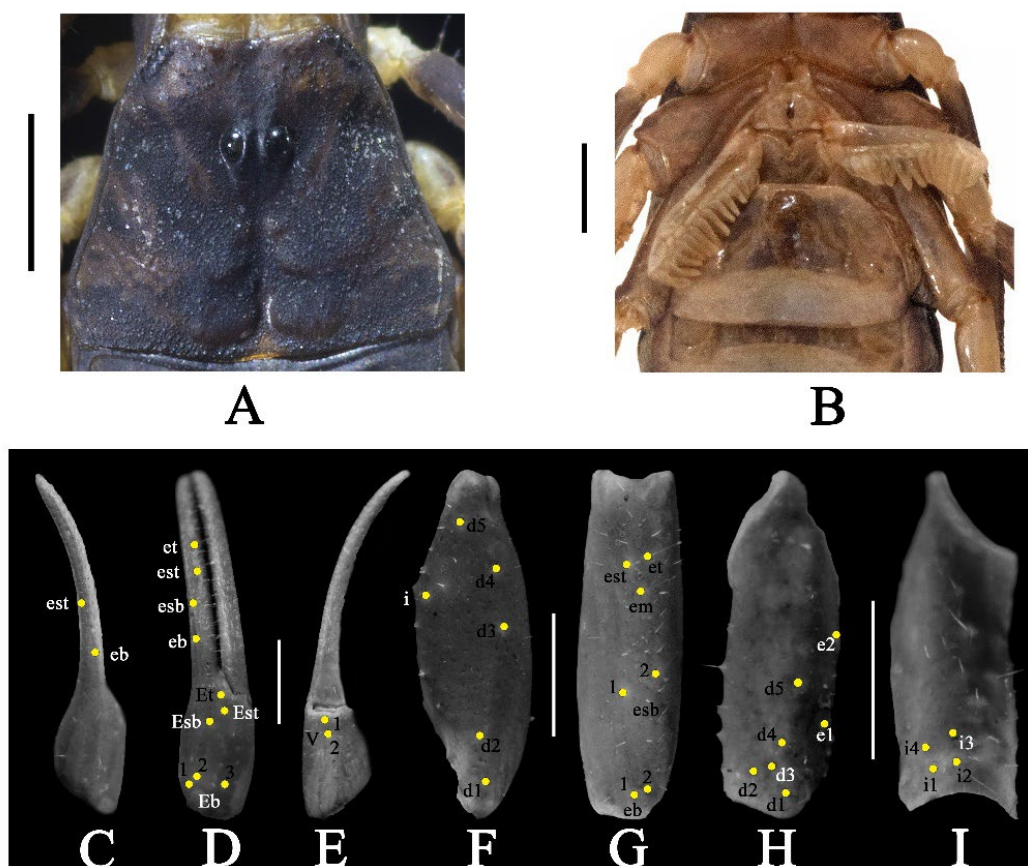

Figure 6. *Charmus sinhagadensis* Tikader & Bastawade, 1983; neotype, adult ♂ (BNHS SC 403); (**A**) aarapace, white light, (**B**) sternopectinal area, (**C–I**) trichobothrial pattern on (**C–E**) chela, (**C**) dorsal view. (**D**) External view, (**E**) ventral view; (**F,G**) patella, (**F**) dorsal view, (**G**) external view; (**H,I**) femur, (**H**) dorsal view, (**I**) internal view. Scale bars: 1 mm.

Legs (Figure 5A,B): femur and patellae carinated. Tibiae III and IV carinated, with long tibial spurs. All legs with a pair of pedal spurs. Tarsomere covered with long delicate setae arranged in parallel rows on ventral side. Tarsomere I (basitarsus) with a tuft of short, stout golden setae on ventral side. Tarsomere II (telotarsus) with a small bulge situated laterally on the proximal portion. Tarsomere II compressed laterally and ventrally with paired row of short, pointed, anteriorly directed, closely placed setae. Tarsomere II with a single row of granular carina on the ventral surface.

Genital operculum (Figure 6B): Wider than long, elliptical, separated by a pair of short male genital papillae.

Pectines (Figures 6B and 16B): basal piece deeply notched on anterior median margin, lateral areas of posterior margin curved anteriorly. Marginal lamella of 3/3 digits and median lamella of 7/7 digits, outer margin armed with a row of stout short golden setae and few setae on surface. Fulcra 17/17, very small, roughly triangular, each armed with few short golden setae, placed in between adjacent pectinal teeth. Teeth 14/16, strong and stout.

Mesosoma (Figure 5A,B): tergites I–VI finely granular with median carina moderately developed throughout. Posterior margin finely crenulated and lateral margins almost smooth. Tergite VII strongly and densely granular, narrowed posteriorly, with two pairs of lateral granular carinae. Sternites III–VI almost smooth, each with a pair of spiracles. Lateral margin of Sternite VI with a pair of weakly granular carinae. Sternite VII with two pairs of weakly developed granular carinae present on two-thirds posterior portion. Intercarinal space strongly and sparsely granular.

Figure 7. Dry deciduous forests around Sinhagad Fort, India; the type locality of *Charmus sinhagadensis* Tikader and Bastawade, 1983. Photo by Mihir Joshi.

Metasoma (Figures 5A,B, 17B, 18B, 19B and 20B): all segments longer than wide. All segments punctate and strongly hairy with few long and few short setae. Segment I with four pairs of granular carinae (dorsal lateral, lateral supramedian, ventral lateral and ventral submedian). Segment II with five pairs of carinae (dorsal lateral, lateral supramedian, lateral inframedian, ventral lateral and ventral submedian). Segment III

with three pairs of carinae (dorsal lateral, ventral lateral and ventral submedian). Dorsal lateral carinae of segment I–III ending posteriorly into a short tubercle. Ventral submedian carina of segment I–III moderately developed. Segment IV acarinate, heavily punctate and hairy. Segment V with a pair of weakly developed dorsal lateral carina present on the anterior portion. Anterior ventral portion of Segment IV and posterior ventral portion of segment V with few scattered granules. Intercarinal surfaces of segments I–II strongly and densely granular, segment III weakly granular. Anal rim with two margins, lower margin moderately crenulated and upper margin weakly crenulated.

Telson (Figures 5A,B, 17B, 18B, 19B and 20B): telson punctate and hairy. Stout and globular without carinae. A depression present on dorsal lateral surface of vesicle. Proximal portion of vesicle with a pair of strongly developed nodule. Aculeus elongated and strongly curved.

Distribution, habitat and ecology (Figure 7): the types of *C. sinhagadensis* were collected from the trail to Sinhagad Fort, Pune, Maharashtra. The individuals were mainly observed scurrying across basaltic boulders while others were found under the dense undergrowth of *Strobilanthes* sp. Blume, 1826 shrubs, which occupy much of the hill slopes in the Northern Western Ghats of Maharashtra. Individuals were actively seen and collected only during the dry seasons between April and June, and their ecology remains unknown.

Remarks:

The authors believe that the holotype of *C. sinhagadensis* (female) (ZSI 5079/18) is lost, as it could not be found in any ZSI centers despite an extensive search. To stabilize the taxonomy of the genus, we found it necessary to designate a neotype using the specimen under the voucher number BNHS SC 403. The neotype meets all the requirements of Article 75 of ICZN as it was collected from the exact type locality and the collected specimens exactly match the descriptions as per Tikader and Bastawade [6].

3.3. Charmus brignolii (Lourenço, 2000)

Figures 8–11 and 15–20, Tables 3 and 4

Holotype (not examined): India, Tamil Nadu, Puducherry, 1899, ♂(MNHN RS-1247). Other material: India, Tamil Nadu, Puducherry, Auroville, 12.0052° N, 79.8069° E, 84 m a.s.l., 26 June 2023, leg. Shauri Sulakhe, Shubhankar Deshpande, Mihir Joshi; 3 ♂(IES 614, IES 615, IES 616), 7 ♀(IES 609, IES 609, IES 610, IES 611, IES 612, IES 613); India, Andhra Pradesh, Nellore District, Sangam town, 14.5900N, 79.7472E, 17m a.s.l., 28 June 2022, leg. Shauri Sulakhe, Shubhankar Deshpande, Rohit Karmalkar;, 3♂(IES 475, IES 479, IES 483), 6 ♀(IES 474, IES 476, IES 477, IES 480, IES 481, IES 482); India, Tamil Nadu, Salem District, Salem, 11°34′36.9″ N 78°02′31.4″ E, 278 m a.s.l., 30 September 2021, leg. Shauri Sulakhe, Shubhankar Deshpande, Rohit Karmalkar, 1 individual (unknown sex) (IES 586).

Description (♂, IES 616, measurements in Tables 3 and 4):

Coloration (Figure 8A,B): body dorsal surface entirely black; legs blackish yellow with tarsomere yellow; metasoma black to dark brown; pedipalp fingers light brown. Ventral surface light yellow except last sternite dark brown. Basal segments of chelicerae yellow with black reticulation ending anteriorly into black transverse patch. Fingers of chelicerae blackish brown with tip of the fingers brown. Telson dark reddish brown in color.

Carapace (Figures 9A and 15C). Surface with mixed and dense granulation. Carapace without carinae. Median supra-ocular area densely granular. Interocular area with mixed and dense granulation. A pair of median eyes situated anteriorly in the ratio 1:1.4 (Ratio of median eyes to anterior margin and median eyes to posterior margin). Antero-lateral ocular tubercle granular with type 3A ocelli. Three well-developed lateral ocelli, all three ocelli of same size. Longitudinal furrow shallow anteriorly and deep posteriorly. Anterior margin finely crenulated in the median portion and slightly curved. Lateral margins smooth below lateral ocelli. Posterior margin almost entirely smooth.

Table 3. Measurements and meristics of *Charmus brignolii* Lourenco, 2000 (in mm).

		IES-614 (♂)	IES-615 (♂)	IES-616 (♂)	IES-611 (♀)	IES-612 (♀)
Carapace	L/W	1.96/1.73	2.09/1.83	2.08/1.87	1.98/1.89	2.08/1.80
Mesosoma	L	4.06	3.97	3.84	2.36	4.67
Tergite VII	L/W	0.92/2.04	0.86/2.04	0.83/2.26	0.55/1.24	1.16/2.33
Metasoma and telson	L	8.47	8.40	9.05	6.05	8.39
Segment I	L/W/D	0.79/1.32/0.96	0.82/1.41/1.1	0.85/1.53/1.04	1.09/1.4/1.19	0.81/1.39/1.06
Segment II	L/W/D	1.05/1.36/0.90	1.13/1.46/1.26	1.2/1.36/1.13	1.19/1.41/1.19	1.07/1.43/1.04
Segment III	L/W/D	1.19/1.42/1.05	1.33/1.54/1.32	1.43/1.48/1.2	1.83/1.41/1.18	1.26/1.45/1.27
Segment IV	L/W/D	1.52/1.42/1.20	1.5/1.51/1.24	1.57/1.62/1.24	1.94/1.41/1.17	1.44/1.57/1.33
Segment V	L/W/D	2.12/1.53/1.12	1.8/1.56/1.21	2.2/1.55/1.15	-	1.8/1.59/1.35
Telson	L/W/D	0.91/0.71/0.83	1.13/0.82/0.76	1.04/0.78/0.90	-	1.14/0.81/0.84
Pedipalp	L	6.47	6.37	6.68	7.42	8.36
Femur	L/W	1.66/0.48	1.68/0.46	1.66/0.47	1.51/0.79	1.71/0.52
Patella	L/W	1.94/0.71	1.95/0.76	2.07/0.74	3.08/1.11	2/0.76
Chela	L	2.87	2.74	2.95	2.83	4.65
Manus	W/D	0.57/0.54	0.56/0.53	0.65/0.59	0.93/0.62	0.58/0.55
Movable finger	L	2	1.64	2.02	1.91	2.01
Pectine	L/W	1.78/0.45	1.77/0.4	1.82/0.41	1.63/0.4	1.97/0.39
Genital Operculum	L/W	0.43/0.54	0.45/0.65	0.38/0.59	0.36/0.64	0.48/0.66
Total	L	14.49	14.46	14.97	10.39	15.14
Pectinal teeth count	PTC	16/16	16/16	17/17	16/17	16/16
		IES-608 (unidentified sex)	IES-609 (♀)	IES-610 (♀)	IES-613 (♀)	IES-617 (♀)
Carapace	L/W	2.04/1.83	2.06/1.75	2.08/1.81	1.87/1.70	1.99/1.83
Mesosoma	L	3.94	4.15	3.81	3.92	3.64
Tergite VII	L/W	0.85/1.65	0.95/2.19	0.83/1.81	0.89/1.89	0.76/1.96
Metasoma and telson	L	8.86	8.63	7.93	8.76	8.54
Segment I	L/W/D	0.83/1.37/1.12	0.8/1.36/1.19	0.81/1.39/1.16	0.9/1.36/1.09	0.82/1.36/1.15
Segment II	L/W/D	1.15/1.4/1.18	1.00/1.4/1.27	1.17/1.37/1.22	1.07/1.44/1.1	1.03/1.44/1.19
Segment III	L/W/D	1.27/1.46/1.24	1.18/1.46/1.39	1.26/1.48/1.32	1.19/1.51/1.22	1.20/1.42/1.22
Segment IV	L/W/D	1.52/1.49/1.23	1.54/1.44/1.39	1.34/1.5/1.3	1.48/1.56/1.14	1.52/1.48/1.24
Segment V	L/W/D	2.22/1.49/1.17	2.25/1.54/1.35	1.73/1.55/1.28	2.22/1.57/1.18	2.18/1.43/1.25
Telson	L/W/D	1.1/0.75/0.84	1.09/0.75/0.89	0.99/0.76/0.79	0.99/0.79/0.96	1/0.71/0.94
Pedipalp	L	6.09	6.42	6.17	6.08	6.16
Femur	L/W	1.61/0.51	1.65/0.51	1.65/0.49	1.6/0.48	1.54/0.53
Patella	L/W	1.77/0.71	1.94/0.75	1.85/0.68	1.89/0.70	1.93/0.75
Chela	L	2.71	2.83	2.67	2.59	2.69
Manus	W/D	0.52/0.61	0.56/0.5	0.57/0.61	0.56/0.6	0.61/0.58
Movable finger	L	2.09	1.84	1.88	1.72	1.96
Pectine	L/W	1.67/0.39	1.57/0.37	1.61/0.4	1.55/0.3	1.55/0.34
Genital Operculum	L/W	0.4/0.59	0.44/0.62	0.44/0.6	0.33/0.68	0.36/0.53
Total	L	14.84	14.84	13.82	14.55	14.17
Pectinal teeth count	PTC	17/17	16/17	16/16	16/17	16/16

Table 4. Measurements and meristics of *Charmus brignolii* Lourenço, 2000 (in mm).

		IES-475 (♂)	IES-479(♂)	IES-483(♂)	IES-474(♀)
Carapace	L/W	2.1/1.85	2.06/1.85	1.64/1.42	1.69/1.49
Mesosoma	L/W	4.55	4.10	2.98	2.48
Tergite VII	L/W	1.13/2.43	0.93/1.95	0.80/1.47	0.7/1.78
Metasoma and telson	L	8.88	8.41	7.59	7.32
Segment I	L/W/D	0.84/1.47/1.26	0.94/1.41/1.11	0.85/1.21/0.98	0.73/1.17/1.03
Segment II	L/W/D	1.15/1.53/1.37	1.12/1.46/1.19	1.00/1.12/1.09	1.01/1.26/1.12
Segment III	L/W/D	1.24/1.58/1.50	1.2/1.5/1.29	1.07/1.2/1.12	1.16/1.2/1.21
Segment IV	L/W/D	1.65/1.6/1.50	1.141/1.52/1.36	1.18/1.26/1.14	1.25/1.22/1.15
Segment V	L/W/D	2.06/1.58/1.51	1.95/1.57/1.42	1.86/1.27/1.16	1.74/1.22/1.13
Telson	L/W/D	1.16/0.89/0.94	1.07/0.82/0.95	0.97/0.68/0.90	0.78/0.66/0.79
Pedipalp	L	6.72	6.48	5.29	4.19
Femur	L/W	1.61/0.59	1.60/0.48	1.34/0.47	0.91/0.43
Patella	L/W	2.09/0.78	1.98/0.77	1.64/0.58	1.02/0.59
Chela	L	3.02	2.90	2.31	2.26
Manus	W/D	0.61/0.64	0.67/0.75	0.47/0.52	0.43/0.47
Movable finger	L	2.08	1.91	1.53	1.56
Pectine	L/W	1.57/0.36	1.46/0.35	1.11/0.26	1.31/0.31
Genital Operculum	L/W	0.28/0.47	0.44/0.58	0.29/0.38	0.32/0.42
Total	L	15.53	14.57	12.21	11.49
Pectinal teeth count	PTC	16/16	15/16	15/17	15/15
		IES-476(♀)	IES-477(♀)	IES-481 (♀)	IES-482 (♀)	IES-586 (unidentidied sex)
Carapace	L/W	1.67/1.41	2.06/1.8	2.14/1.9	1.65/1.4	1.88/1.70
Mesosoma	L/W	3.03	6.21	4.26	2.62	3.23
Tergite VII	L/W	0.8/1.45	1.18/2.37	0.93/2.24	0.72/1.57	0.91/1.8
Metasoma and telson	L	7.40	8.70	9.39	7.11	8.42
Segment I	L/W/D	0.67/1.05/0.98	0.69/1.47/1.27	0.91/1.43/1.26	0.73/1.19/0.93	0.83/1.15/1.06
Segment II	L/W/D	0.9/1.12/1.01	1.35/1.5/1.32	1.12/1.32/1.22	0.96/1.14/0.93	1.12/1.11/1.08
Segment III	L/W/D	0.96/1.16/1.04	1.44/1.58/1.39	1.31/1.51/1.32	1.00/1.81/1.14	1.19/1.16/1.07
Segment IV	L/W/D	1.36/1.22/1.05	1.49/1.53/1.42	1.61/1.47/1.45	1.06/1.18/1.15	1.48/1.13/1.05
Segment V	L/W/D	2.01/1.23/1.13	1.96/1.62/1.27	2.26/1.56/1.44	1.71/1.16/0.99	1.91/1.17/1.04
Telson	L/W/D	0.89/0.64/0.74	1.17/0.82/0.96	1.09/0.85/0.96	0.96/0.63/0.78	1.1/0.79/0.86
Pedipalp	L	4.86	6.05	5.98	4.76	5.98
Femur	L/W	1.31/0.43	1.75/0.55	1.62/0.51	1.16/0.51	1.6/0.44
Patella	L/W	1.48/0.53	1.87/0.78	1.69/0.7	1.53/0.57	1.86/0.63
Chela	L	2.07	2.43	2.67	2.07	2.52
Manus	W/D	0.43/0.45	0.60/0.63	0.58/0.63	0.39/0.45	0.49/0.54
Movable finger	L	1.50	2.00	1.8	1.44	1.93
Pectine	L/W	1.59/0.40	1.76/0.35	1.62/0.37	1.31/0.32	1.66/0.32
Genital Operculum	L/W	0.32/0.47	0.47/0.62	0.45/0.57	0.29/0.57	0.32/0.48
Total	L	12.1	16.97	15.79	11.38	13.53
Pectinal teeth count	PTC	16/17	18/16	16/16	16/15	-

Chelicerae: characteristic of the family Buthidae. Basal segments and movable fingers with tuft of short and firm setae on ventral surfaces. Dorsal surfaces smooth.

Pedipalp (Figure 8A,B, Figure 9C–I and Figure 10C): femur with five carinae (prodorsal, retrodorsal, promedian, proventral and retroventral). All carinae crenulated. Intercarinal surfaces with mixed and dense granulation except ventral surface smooth with a few fine granules on proximal portions. Patella almost smooth without developed carinae except promedian carina moderately developed with 7 spinoid granules. Intercarinal surface almost smooth. Manus smooth without carinae. Fixed fingers acarinate. Movable and fixed fingers with eight oblique rows of granules, each row (except most proximal) with one internal accessory granule. Trichobothrial pattern of type Aα, typical for the genus (chela dorsal 2, chela retrolateral 10, chela ventral 2, patella dorsal 6, patella retrolateral 7, femur dorsal 7 and femur prolateral 4).

Legs (Figure 8A,B): femur and patellae carinated. Tibiae III and IV carinated, with long tibial spurs. All legs with a pair of pedal spurs. Tarsomere covered with long delicate setae arranged in parallel rows on ventral side. Tarsomere I (basitarsus) with a tuft of short, stout golden setae on ventral side. Tarsomere II (telotarsus) with a small bulge situated laterally on the proximal portion. Tarsomere II compressed laterally and ventrally with a paired row of short, pointed, anteriorly directed, closely placed setae. Tarsomere II with a single row of granular carina on the ventral surface.

Figure 8. *Charmus brignolii* Lourenço, 2000; adult ♂(IES-616); (**A**) dorsal view (**B**) ventral view. Scale bar: 5 mm.

Pectines (Figures 9B and 16C): basal piece moderately notched on anterior median margin, lateral areas of posterior margin almost straight. Marginal lamella of 3/3 digits

and median lamella of 6/6 digits, outer margin armed with a row of stout short golden setae and few setae on surface. Fulcra 16/16, very small, roughly triangular, each armed with few short golden setae, placed in between adjacent pectinal teeth. Teeth 17/17, strong and stout.

Mesosoma (Figure 8A,B): tergites I–VI coarsely granular with median carina moderately developed throughout, except vestigial on first segment. Posterior margin strongly crenulated and lateral margins almost smooth. Tergite VII strongly and densely granular, narrowed posteriorly, with two pairs of lateral granular carinae. Sternites III–VI smooth, each with a pair of spiracles. Sternite VII acarinate with scattered strong and sparse granules.

Genital operculum (Figure 9B): wider than long, elliptical, separated by a pair of short male genital papillae.
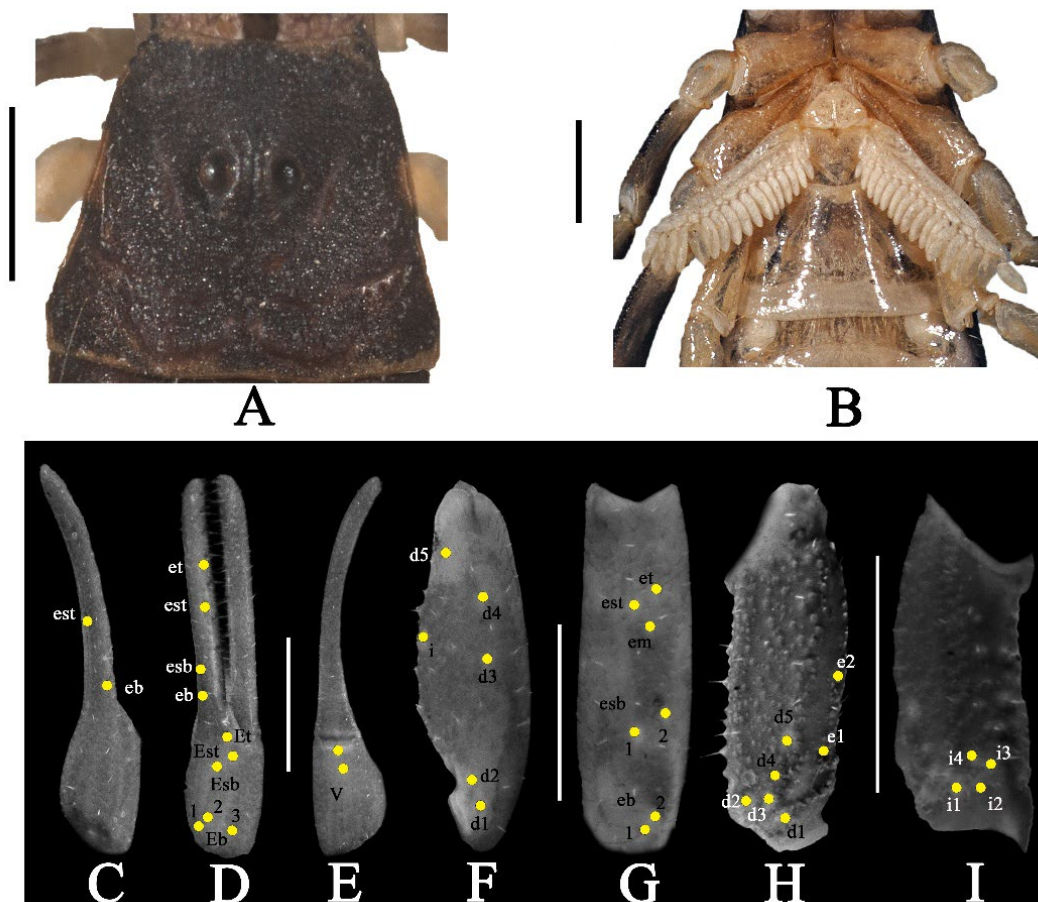
Figure 9. *Charmus brignolii* Lourenço, 2000; adult ♂ (IES-616); (**A**) carapace, white light (**B**) sternopectinal area, (**C**–**I**) trichobothrial pattern on (**C**–**E**) chela, (**C**) dorsal view. (**D**) External view, (**E**) ventral view; (**F**,**G**) patella, (**F**) dorsal view, (**G**) external view; (**H**,**I**) femur, (**H**) dorsal view, (**I**) internal view. Scale bars: 1 mm.

Metasoma (Figure 8A,B, Figures 17C, 18C, 19C and 20C): all segments longer than wide except Segment I wider than long. All segments punctate and strongly hairy with few long and few short setae. Segment I with four pairs of granular carinae (dorsal lateral, lateral supramedian, ventral lateral and ventral submedian). Segment II with five pairs of carinae (dorsal lateral, lateral supramedian, lateral inframedian, ventral lateral and ventral submedian). Segment III with three pairs of carinae (dorsal lateral, ventral lateral and ventral submedian). Dorsal lateral carinae of segment I–III ending posteriorly into a short tubercle. Ventral submedian carina of segment I–III strongly developed. Segment IV and V

heavily punctate and hairy. Segment IV with a pair of strongly developed dorsal lateral carina present on the anterior portion. Segment V with a pair of strongly developed dorsal lateral carina present on the anterior portion. Anterior ventral portion of Segment IV and posterior ventral portion of segment V with few scattered granules. Intercarinal surfaces of segments I–III strongly and densely granular. Anal rim with two margins, lower margin moderately crenulated and upper margin weakly crenulated.
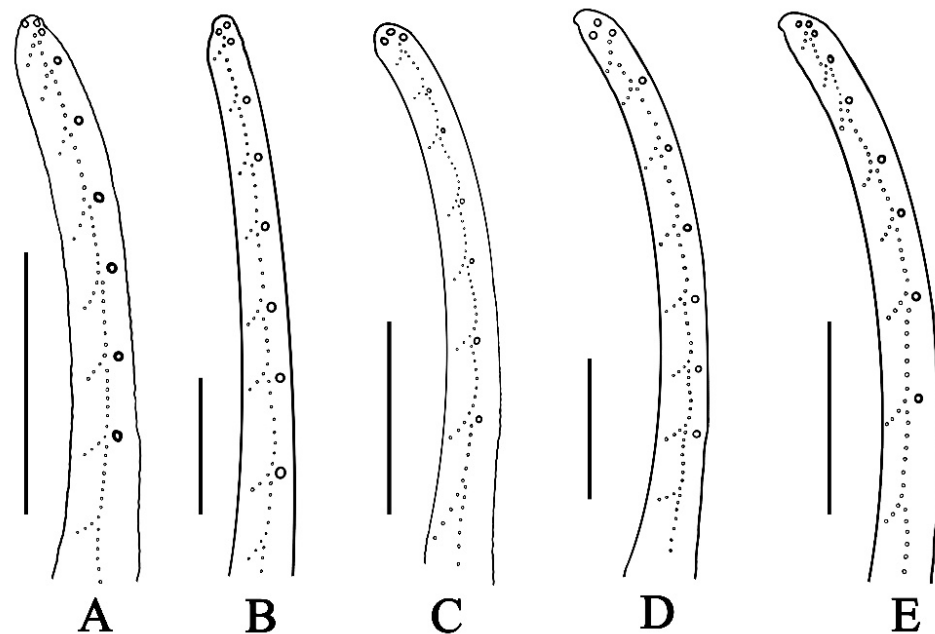

Figure 10. Illustration showing number of rows of granules on movable finger of pedipalp chela; (**A–E**); (**A**) *Charmus laneus* Karsch, 1879, adult ♂(IES-631); (**B**) *Charmus sinhagadensis* Tikader & Bastawade, 1983; neotype, adult ♂(BNHS SC 403); (**C**) *Charmus brignolii* Lourenço, 2000; adult ♂(IES-616); (**D**) *Charmus dakshini* sp. nov.; holotype, adult ♂(BNHS SC 404), (**E**) *Charmus saradieli* Kovarik et al. 2016 adult ♂(Locality 18 CO) from Sri Lanka. Scale bars: 1 mm. Illustrations by Rohit Karmalkar.

Telson (Figure 8A,B, Figures 17C, 18C, 19C and 20C): telson punctate and hairy. Stout and globular without carinae. A depression present on dorsal lateral surface of vesicle. Proximal portion of vesicle with a pair of moderately developed nodules. Aculeus elongated and strongly curved.

Distribution, habitat, and ecology (Figure 11): specimens of *C. brignolii* were collected from the low-lying coastal plains of Auroville, Puducherry, India. The individuals were observed active at night, hiding under leaf litter or grass.

Remarks:

Reddy [9], in his redescription of *C. indicus*, cites a male specimen collected from Puducherry around the year 1900, which was deposited at the MNHN. The same individual was identified as *C. annulipes* by E. Simon and finally described by Lourenço [6] as *Charmus brignolii*. Several of the differences that Lourenço used to separate *C. indicus* from *C. brignolii* such as overall granulation on the body, hairiness of metasomal segments, the number of rows of granules on the movable finger of the chela, the nature of the median carina on the tergites, the size of the lateral eyes, and the presence of spinoid granules on the promedian carina of the patella seem rather arguable given the high amounts of morphological plasticity within the genus.

We examined multiple specimens of *C. brignolii* from various localities and compared them with all the existing *Charmus* species from India. All populations showed significant intraspecific variation in characters like the size of lateral eyes, hairiness of metasoma, nature of median carina on tergites, and the number of spinoid granules on promedian

carina of the patella. The only character of importance that showed significant stability throughout the examined material is the number of rows of granules on the pedipalp chela, which happens to be constant across all known species of *Charmus* (Figure 10, Table S6).

These findings demonstrate that the character diagnosis used by Lourenço to separate *C. brignolii* from *C. laneus* is inaccurate because the intraspecific variation was not taken into account. Nevertheless, *C. brignolii* remains a valid species, exhibiting few but reliable morphological differences, such as median supra ocular region densely granular and mesosomal tergites I–VI coarsely granular (characters that were not recognized as diagnostically important by Lourenço), as well as significant molecular divergence from *C. laneus.*

In his description, Lourenço explicitly mentions that the exact geographic locality of *C. brignolii* is unknown, as Puducherry functioned as a French trading post, where goods were typically packaged and shipped to France. Therefore, the type specimen of *C. brignolii* could have been collected anywhere in India before being shipped to France from Puducherry. In order to remove this ambiguity, we consider that among the localities where the species has been collected (Sangam, Andhra Pradesh and Salem), Auroville (12.0052° N, 79.8069° E) is the closest to Puducherry and therefore the most appropriate proxy for the type locality of *Charmus brignolii* Lourenco, 2000.

Figure 11. Dry scrubland around Aurovile, Puducherry from where *Charmus brignolii* Lourenço, 2000 were collected. Photo by Neil Kakkar.

3.4. Charmus dakshini sp. nov.

urn:lsid:zoobank.org:pub:4DD30BD9-355F-4837-9053-C51489896E88

Figures 12–20, Tables 5 and 6

Table 5. Measurements and meristics of *Charmus dakshini* sp. nov. from Sirumalai (in mm).

		BNHS SC-404 (♂)	IES-624 (♂)	IES-626 (♂)	IES-627 (♂)
		Holotype	Paratype	Paratype	Paratype
Carapace	L/W	2.15/1.84	2.09/1.75	2.01/1.77	2.09/1.74
Mesosoma	L	3.68	3.61	3.18	3.63
Tergite VII	L/W	1.06/1.80	1.01/1.9	0.92/1.85	1.04/1.8
Metasoma and telson	L	9.46	8.93	9.50	5.53
Segment I	L/W/D	1.01/1.36/0.93	1.08/1.37/1.18	1.1/1.35/0.94	1.07/1.31/0.9
Segment II	L/W/D	1.05/1.33/0.94	1.11/1.36/1.25	1.17/1.3/1.08	1.04/1.31/0.98
Segment III	L/W/D	1.31/1.38/1.06	1.29/1.37/1.33	1.37/1.34/1.13	1.24/1.3/1.08
Segment IV	L/W/D	1.62/1.36/1.04	1.59/1.35/1.35	1.62/1.35/1.15	-
Segment V	L/W/D	2.41/1.35/1.07	1.87/1.33/1.25	2.14/1.35/1.16	-
Telson	L/W/D	1.15/0.79/0.95	1.27/0.97/0.94	1.32/0.84/0.92	1.35/0.94/0.98
Pedipalp	L	6.97	7.88	6.48	6.76
Femur	L/W	1.81/0.58	2.03/0.64	1.8/0.57	1.68/0.64
Patella	L/W	2.19/0.79	2.37/0.92	2.16/0.76	2.12/0.89
Chela	L	2.97	3.48	2.52	2.96
Manus	W/D	0.62/0.70	0.70/0.62	0.61/0.64	0.64/0.74
Movable finger	L	1.90	2.02	1.88	2.36
Pectine	L/W	1.98/0.4	2.07/0.41	1.91/0.38	1.22/0.44
Genital Operculum	L/W	0.38/0.7	0.32/0.53	0.37/0.55	0.32/0.34
Total	L	15.29	14.63	14.69	11.25
Pectinal teeth count	PTC	18/18	18/18	18/19	18/19
		IES-385 (♂)	**IES-621 (♀)**	**IES-622 (♀)**	**IES-623 (♀)**	**IES-386 (♀)**
		Paratype	Paratype	Paratype	Paratype	Paratype
Carapace	L/W	2.01/1.88	2.04/1.76	2.01/1.78	1.95/1.7	2.23/1.66
Mesosoma	L	4.36	4.40	3.15	3.34	4.07
Tergite VII	L/W	1.19/1.80	1.1/1.73	0.86/1.99	0.94/1.78	1.13/2.02
Metasoma and telson	L	9.01	9.50	8.40	8.56	10.05
Segment I	L/W/D	0.84/1.31/1.19	1.02/1.28/1.02	0.91/1.18/1.28	0.82/1.26/1.23	1.03/1.44.1.33
Segment II	L/W/D	1.06/1.22/1.13	1.15/1.25/1.04	1.01/1.29/1.29	0.98/1.26/1.16	1.22/1.43/1.3
Segment III	L/W/D	1.4/1.23/1.17	1.34/1.28/1.04	1.16/1.26/1.31	1.15/1.23/1.31	1.38/1.4/1.35
Segment IV	L/W/D	1.53/1.23/1.16	1.66/1.38/1.04	1.37/1.33/1.35	1.49/1.26/1.3	1.66/1.42/1.33
Segment V	L/W/D	2.25/1.28/1.12	2.1/1.36/1.04	2.15/1.35/1.21	2.17/1.28/1.25	2.70/1.57/1.26
Telson	L/W/D	1.09/0.77/0.9	1.41/0.85/1.00	1.2/0.85/0.99	1.21/0.77/0.94	1.18/0.98/1.21
Pedipalp	L	6.77	7.09	6.64	6.42	7.37
Femur	L/W	1.65/0.51	1.85/0.59	1.76/0.54	1.67/0.54	1.99/0.64
Patella	L/W	2.14/0.68	2.21/0.79	2.10/0.72	1.95/0.75	2.28/0.92
Chela	L	2.98	3.03	2.78	2.80	3.10
Manus	W/D	0.54/0.58	0.62/0.59	0.61/0.58	0.6/0.61	0.73/0.71
Movable finger	L	1.76	2.15	2.16	2.10	2.47
Pectine	L/W	1.86/0.37	2.01/0.41	1.74/0.31	1.82/0.32	2.05/0.47
Genital Operculum	L/W	0.37/0.53	0.44/0.64	0.41/0.58	0.37/0.61	0.37/0.68

Table 5. *Cont.*

		BNHS SC-404 (♂)		IES-624 (♂)	IES-626 (♂)	IES-627 (♂)
Total	L	15.38	15.94	13.56	13.85	16.35
Pectinal teeth count	PTC	-	18/19	18/18	17/18	18/18

Holotype: India, Tamil Nadu, Sirumalai, Sirumalai Road, 10.1942° N, 77.9967° E, 1600 m a.s.l., 27 June 2023, leg. Shauri Sulakhe, Shubhankar Deshpande, Mihir Joshi; Holotype ♂(BNHS SC 404). Paratypes: Same data as holotype, 3♂(IES 624, IES 626, IES 627), 3♀(IES 621, IES 622, IES 623); 28 September 2021, leg. Shauri Sulakhe, Shubhankar Deshpande, Mukta Nachare, 1♂(IES 385), 1♀(IES 386). Other material examined: India, Tamil Nadu, Palani Hills, Palani-Kodaikanal Road, 10.36° N 77.54° E, 813 m a.s.l., 26th October 2023, leg. Shauri Sulakhe, Shubhankar Deshpande, Mihir Joshi, 2♂(IES 618, IES 619), 2♀(IES 620, IES 621), 30 September 2021, Shauri Sulakhe, Shubhankar Deshpande, Mukta Nachare, 1♀(IES 401).

Etymology: the specific epithet is derived from the Sanskrit word "Dakshin" (=south) indicating the distribution of the species in the southernmost regions of India. It is an invariable noun in apposition.

Description: (♂holotype, BNHS SC-404, measurements in Tables 5 and 6).

Table 6. Measurements and meristics of *Charmus dakshini* sp. nov. from Palani Hills (in mm).

		IES-618 (♂)	IES-619 (♂)	IES-620 (♀)	IES-401 (♀)
		Paratype	Paratype	Paratype	Paratype
Carapace	L/W	2.22/1.85	1.96/1.64	2.03/1.73	2.1/2.06
Mesosoma	L	3.96	3.20	3.69	3.27
Tergite VII	L/W	1.05/2.06	0.9/1.71	1/1.79	0.95/1.93
Metasoma and telson	L	9.93	9.09	9.53	7.88
Segment I	L/W/D	1.25/1.47/1.22	1.13/1.18/1.05	1.01/1.24/1.23	1.13/1.32/1.22
Segment II	L/W/D	1.28/1.41/1.23	1.17/1.16/1.06	1.2/1.14/1.2	1.41/1.29/1.22
Segment III	L/W/D	1.46/1.39/1.27	1.24/1.17/1.05	1.36/1.2/1.24	1.47/1.32/1.21
Segment IV	L/W/D	1.52/1.42/1.22	1.38/1.2/1.05	1.58/1.24/1.2	1.61/1.3/1.22
Segment V	L/W/D	2.38/1.46/1.23	2.18/1.19/1.08	2.34/1.27/1.14	2.26/1.32/1.21
Telson	L/W/D	1.29/0.84/1.03	1.21/0.77/0.91	1.26/0.77/0.93	-
Pedipalp	L	7.23	5.69	7.14	6.86
Femur	L/W	1.80/0.58	1.53/0.51	1.69/0.55	1.63/0.56
Patella	L/W	2.25/0.85	1.78/0.68	2.35/0.75	2.10/0.76
Chela	L	3.18	2.38	3.10	3.13
Manus	W/D	0.64/0.65	0.53/0.56	0.59/0.58	0.63/0.63
Movable finger	L	2.00	2.15	2.14	2.10
Pectine	L/W	2.07/0.41	1.79/0.40	1.7/0.33	1.97/0.42
Genital Operculum	L/W	0.37/0.57	0.38/0.58	0.35/0.54	0.35/0.52
Total	L	16.11	14.25	15.25	13.25
Pectinal teeth count	PTC	18/17	19/19	16/17	19/19

Coloration (Figure 12A–D): body dorsal surface entirely dark brownish to blackish; legs dark brown with tarsomere yellowish brown; metasoma dark brownish to blackish; pedipalp fingers dark brown. Ventral surface brown except last sternite dark brown. Basal segments of chelicerae dark brown with black reticulation ending anteriorly into black

transverse patch. Fingers of chelicerae blackish brown with tip of the fingers brown. Telson dark reddish brown in color.
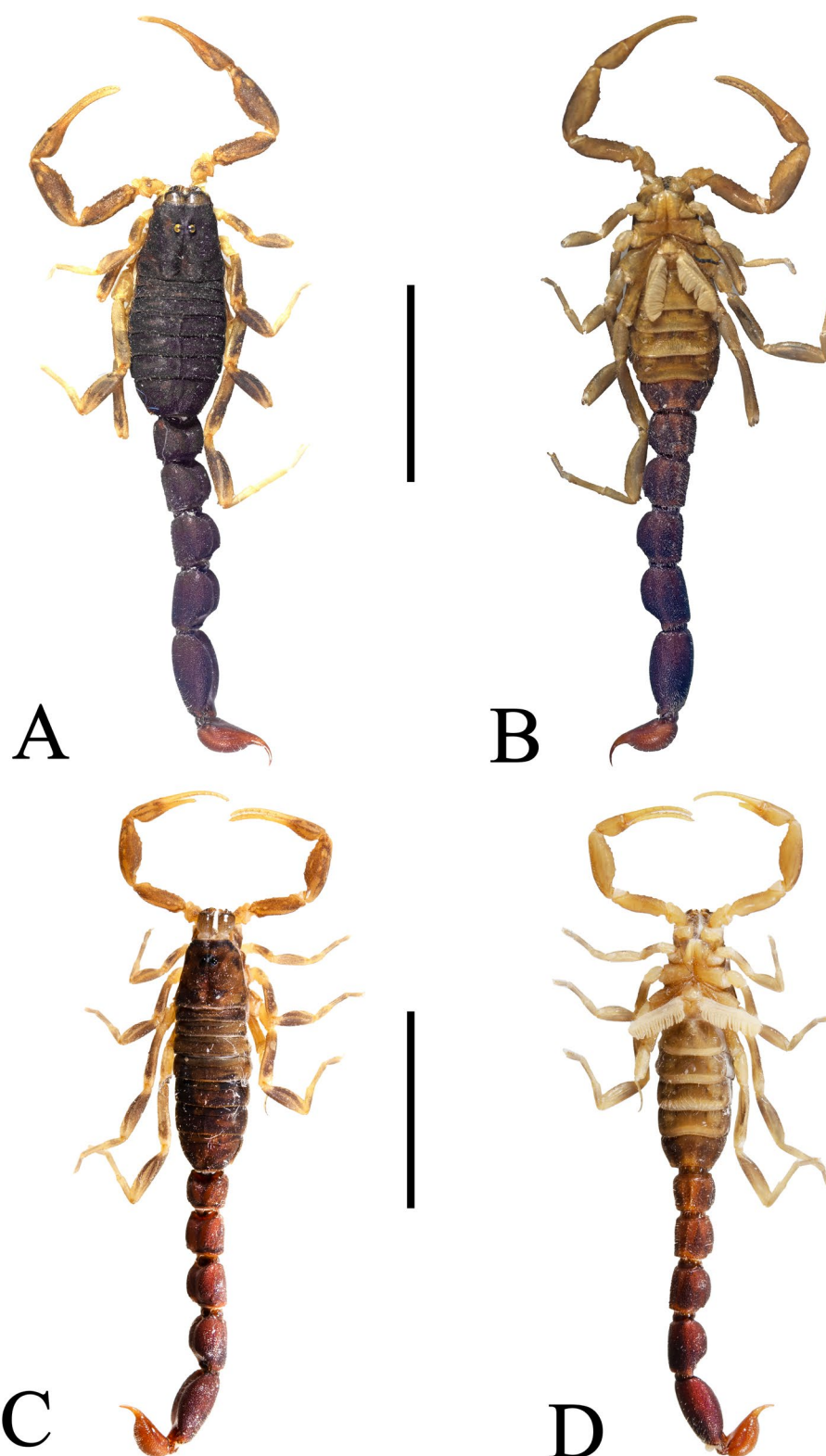
Figure 12. *Charmus dakshini* sp. nov. holotype, adult ♂(BNHS SC 404); (**A**) dorsal view (**B**) ventral view; paratype, adult ♀(IES-621); (**C**) dorsal view, (**D**) ventral view. Scale bars: 5 mm.

Carapace (Figure 13A,B and Figure 15D): surface finely and densely granular. Carapace without carinae. Median supra-ocular area with few sparse granules. Interocular area finely

and densely granular. A pair of median eyes situated anteriorly in the ratio 1:2.3 (ratio of median eyes to anterior margin and median eyes to posterior margin). Antero-lateral ocular tubercle granular with type 3A ocelli. Three well developed lateral ocelli with first and third ocelli smaller than the second ocelli. Longitudinal furrow shallow anteriorly and deep posteriorly. Anterior margin finely crenulated in the median portion and slightly curved. Lateral margins weakly crenulated below lateral ocelli. Posterior margin almost entirely smooth.
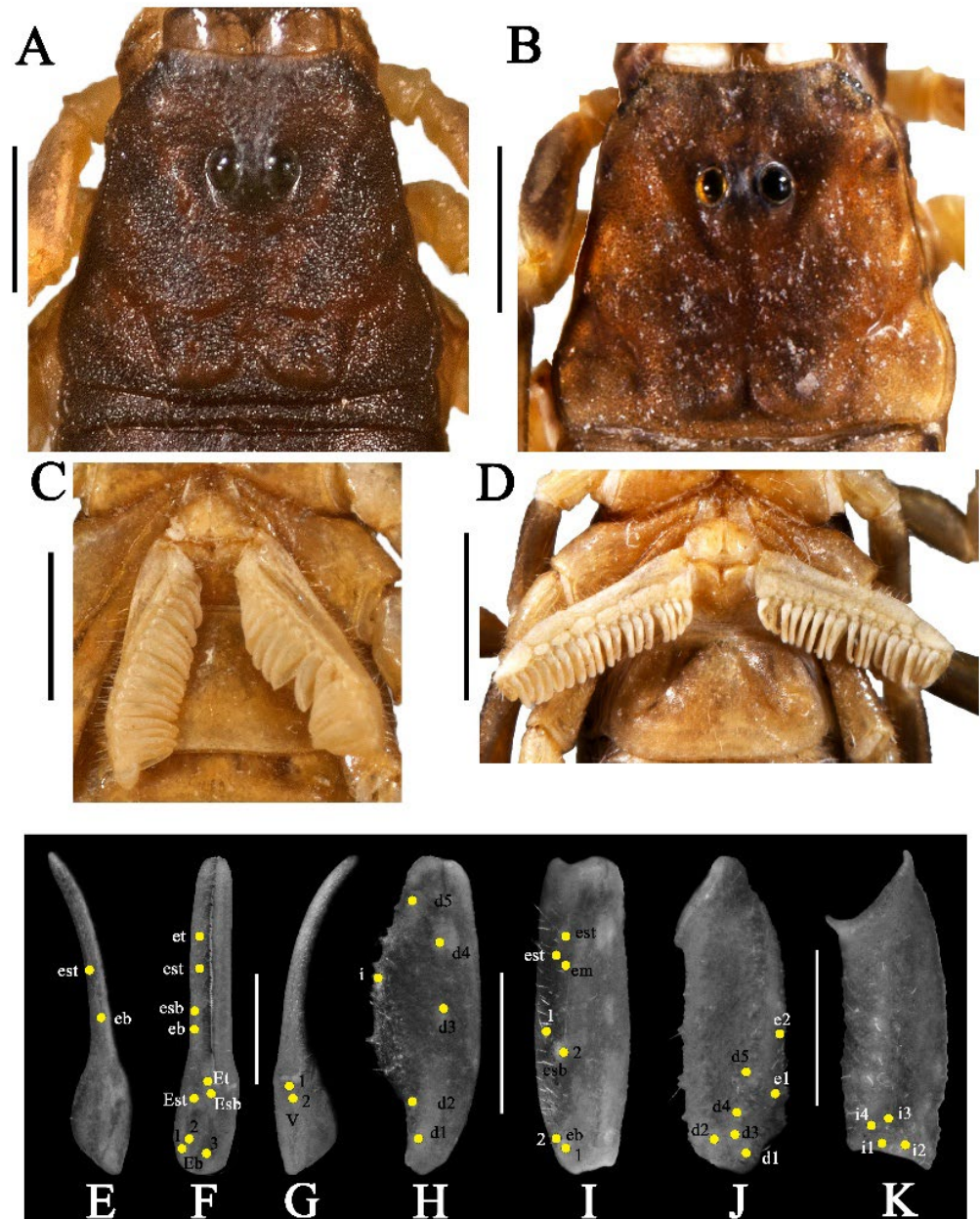
Figure 13. *Charmus dakshini* sp. nov. holotype, adult ♂ (BNHS SC 404); (**A–C**); (**A**) carapace, white light, (**C**) sternopectinal area. (**B–D**) Paratype, adult ♀(IES-621); (**B**) carapace, white light, (**D**) sternopectinal area; (**E–K**) trichobothrial pattern on (**E–G**) chela, (**E**) dorsal view. (**F**) External view, (**G**) ventral view; (**H,I**) patella, (**H**) dorsal view (**I**).

Chelicerae: characteristic of the family Buthidae. Basal segments and movable fingers with tuft of short and firm setae on ventral surfaces. Dorsal surfaces smooth.

Pedipalp (Figures 12A–D and 13E–K): femur with five carinae (prodorsal, retrodorsal, promedian, proventral and retroventral). All carinae crenulated. Intercarinal surfaces with

mixed and sparse granulation except ventral surface smooth with a few fine granules on proximal portions. Patella almost smooth without developed carinae except promedian carina moderately developed with 7 spinoid granules. Intercarinal surfaces almost smooth. Manus smooth without carinae. Fixed fingers acarinate. Movable and fixed fingers with eight oblique rows of granules, each row (except most proximal) with one internal accessory granule. Trichobothrial pattern of type Aα, typical for the genus (chela dorsal 2, chela retrolateral 10, chela ventral 2, patella dorsal 6, patella retrolateral 7, femur dorsal 7 and femur prolateral 4).

Legs (Figure 12A–D): femur and patellae carinated. Tibiae III and IV carinated, with long tibial spurs. All legs with a pair of pedal spurs. Tarsomere covered with long delicate setae arranged in parallel rows on ventral side. Tarsomere I (basitarsus) with a tuft of short, stout golden setae on ventral side. Tarsomere II (telotarsus) with a small bulge situated laterally on the proximal portion. Tarsomere II compressed laterally and ventrally with paired row of short, pointed, anteriorly directed, closely placed setae. Tarsomere II with a single row of granular carina on the ventral surface.

Genital operculum (Figure 13C,D): wider than long, elliptical, separated with a pair of short male genital papillae.

Pectines (Figures 13C,D and 16D): basal piece deeply notched on anterior median margin, lateral areas of posterior margin curved anteriorly. Marginal lamella of 3/3 digits and median lamella of 7/7 digits, outer margin armed with a row of stout short golden setae and few setae on surface. Fulcra 17/17, very small, roughly triangular, each armed with few short golden setae, placed in between adjacent pectinal teeth. Teeth 18/18, strong and stout.

Mesosoma (Figure 12A–D): tergites I–VI finely granular with median carina moderately developed throughout except vestigial on the first segment. Posterior margin finely crenulated and lateral margins almost smooth. Tergite VII strongly and densely granular, narrowed posteriorly, with two pairs of lateral granular carinae. Sternites III–VI almost smooth, each with a pair of spiracles. Sternite VII with two pairs of weakly developed granular carinae present on two-thirds posterior portion. Intercarinal space strongly and sparsely granular.

Metasoma (Figures 12A–D, 17D, 18D, 19D and 20D): all segments longer than wide. All segments punctate and strongly hairy with few long and few short setae. Segment I with five pairs of granular carinae (dorsal lateral, lateral supramedian, lateral inframedian, ventral lateral and ventral submedian). Segment II with four pairs of carinae (dorsal lateral, lateral supramedian, ventral lateral and ventral submedian). Segment III with two pairs of carinae (dorsal lateral and ventral submedian). Dorsal lateral carinae of Segment I–III ending posteriorly into a short tubercle. Ventral submedian carina of Segment I–III weakly developed. Segment IV–V acarinated, heavily punctate and hairy. Intercarinal surfaces of Segments I–II strongly and densely granular, segment III weakly granular. Anal rim with two margins, both lower margin and upper margin weakly crenulated.

Telson (Figures 12A–D, 17D, 18D, 19D and 20D): telson punctate and hairy. Stout and globular without carinae. A depression present on dorsal lateral surface of vesicle. Proximal portion of vesicle with a pair of weakly developed nodule. Aculeus elongated and strongly curved.

Distribution, habitat and ecology (Figure 14): specimens of *Charmus dakshini* sp. nov. were observed to be active at night, usually scurrying across open soil or under dense undergrowth. The species was also observed on Palani-Kodaikanal Road, Palani Hills, Tamil Nadu, about 50 km west from the type locality.
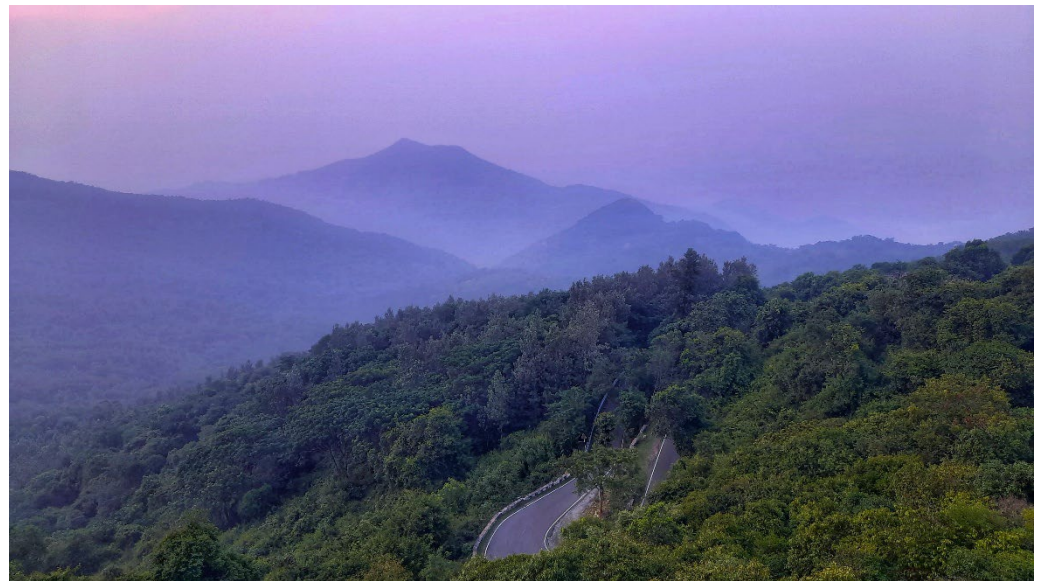
Figure 14. Dense evergreen forests of Sirumalai, India; the type locality of *Charmus dakshini* sp. nov. Photo by Mihir Joshi.

3.5. Affinities (Figures 2, 3, 5, 6, 8–10, 12, 13 and 15–20)

Species of the genus *Charmus* can be differentiated by the following combination of characters:

1. Surface of carapace finely and densely granular in *C. sinhagadensis* (Figures 6A and 15B) and *C. dakshini* sp. nov. (Figures 13A and 15D) as opposed to surface with mixed and dense granulation in *C. laneus* (Figures 3A and 15A,E)*, C. brignolii* (Figures 9A and 15C) and *C. saradieli* (Figure 15F).
2. Anterior margin of carapace finely crenulated in the median portion in *C. laneus* (Figures 3A and 15A,E), *C. brignolii* (Figures 9A and 15C), *C. saradieli* (Figure 15F), and *C. dakshini* sp. nov. (Figures 13A and 15D) as opposed to smooth throughout in *C. sinhagadensis* (Figures 6A and 15B).
3. Dorsal surface of pedipalp patella granular in *C. brignolii* (Figure 9F) as opposed to almost smooth in *C. laneus* (Figure 3F), *C. sinhagadensis* (Figure 6F), *C. saradieli* and *C. dakshini* sp. nov. (Figure 13F).
4. Basal piece of pectines deeply notched on anterior median margin in *C. sinhagadensis* (Figure 16B), *C. saradieli* and *C. dakshini* sp. nov. (Figure 16D) as opposed to moderately notched in *C. laneus* (Figure 16A) and *C. brignolii* (Figure 16C).
5. Tergites I–VI finely granular in *C. sinhagadensis* (Figure 5A) and *C. dakshini* sp. nov. (Figure 12A), as opposed to tergites with mixed granulation in *C. laneus* (Figure 2A) and coarsely granular in *C. brignolii* (Figure 8A) and *C. saradieli*.
6. Ventral submedian carina of metasomal segment (Figure 19) I–III weakly developed in *C. dakshini* sp. nov. as opposed to moderately developed in *C. sinhagadensis* and strongly developed in *C. laneus C. brignolii* and *C. saradieli*.
7. Metasomal segment V acarinate (Figures 17–20) in *C. dakshini* sp. nov. as opposed to segment with a pair of weakly developed dorsal lateral carina present on the proximal portion in *C. saradieli*, moderately developed and present on the proximal portion in *C. sinhagadensis* and strongly developed and present on the proximal portion in *C. laneus* and *C. brignolii*.
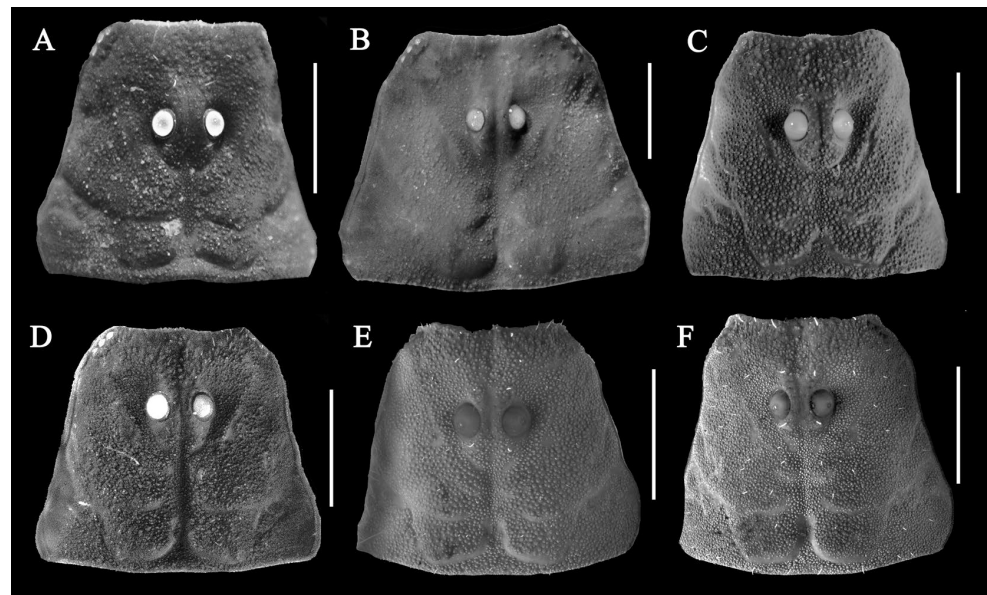
Figure 15. Carapace dorsal views under UV light. (**A**) *Charmus laneus* Karsch, 1879, adult ♂(IES-631); (**B**) *Charmus sinhagadensis* Tikader & Bastawade, 1983; neotype, adult ♂(BNHS SC 403); (**C**) *Charmus brignolii* Lourenço, 2000; adult ♂(IES-616); (**D**) *Charmus dakshini* sp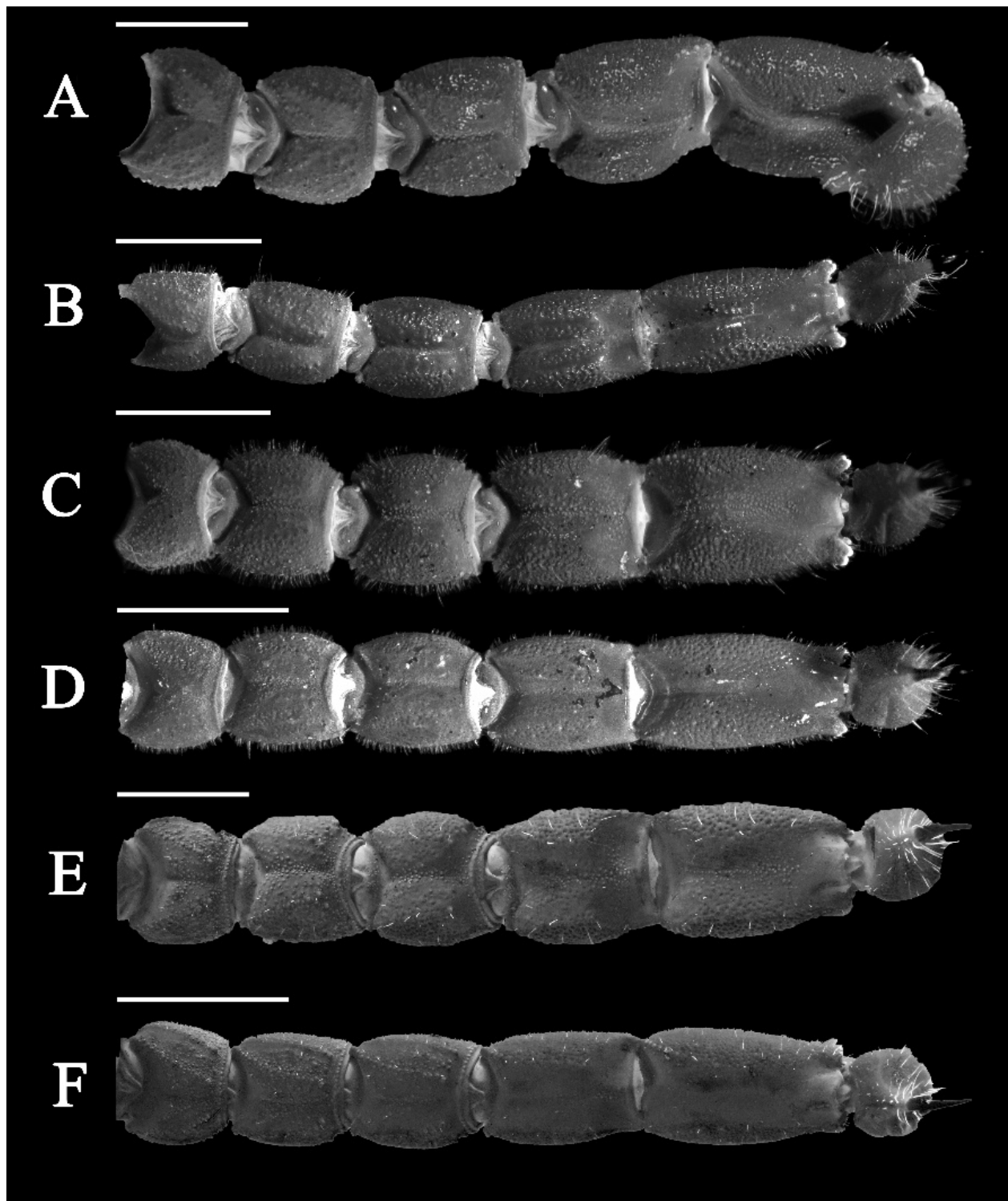. nov.; holotype, adult ♂(BNHS SC 404), (**E**) *Charmus laneus* Karsch, 1879; adult ♂(Locality 15CN) from Sri Lanka; (**F**) *Charmus saradieli* Kovarik et al. 2016 adult ♂(Locality 18 CO) from Sri Lanka. Scale bars: 1 mm.
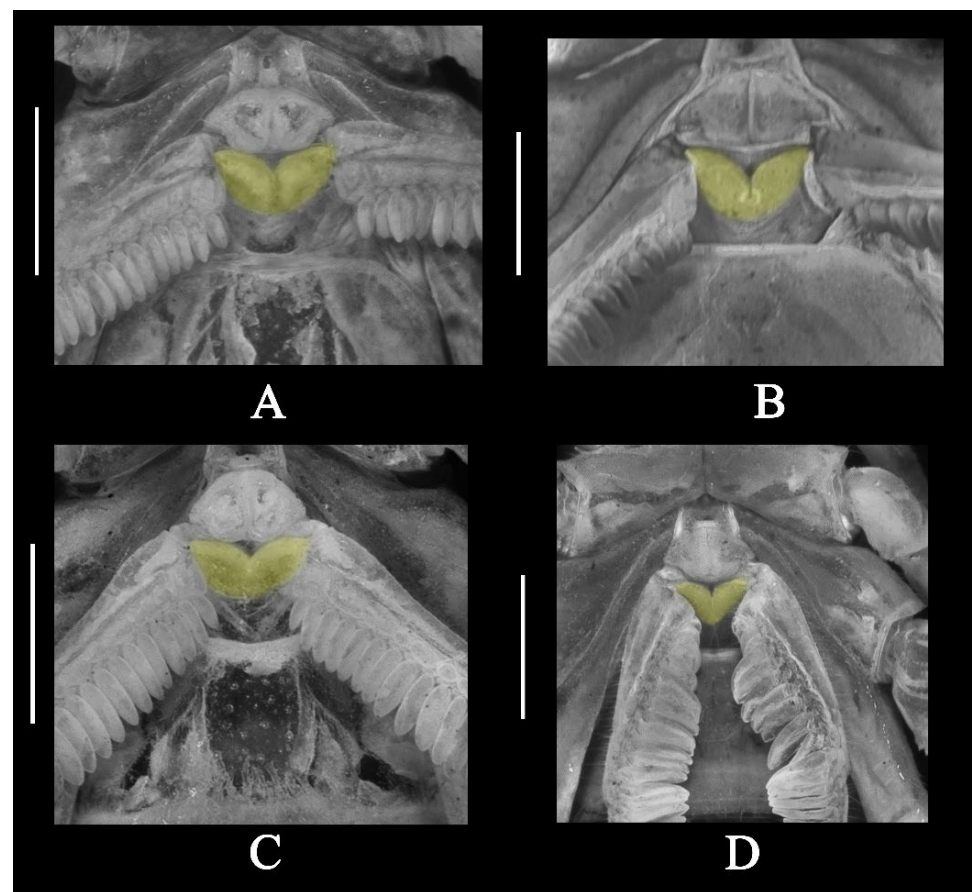
Figure 16. Sternopectinal area under UV light; basal piece highlighted in yellow. (**A**) *Charmus laneus* Karsch, 1879, adult ♂(IES-631); (**B**) *Charmus sinhagadensis* Tikader & Bastawade, 1983; neotype, adult ♂(BNHS SC 403); (**C**) *Charmus brignolii* Lourenço, 2000; adult ♂(IES-616); (**D**) *Charmus dakshini* sp. nov.; holotype, adult ♂(BNHS SC 404).

Figure 17. Metasomal segments dorsal view under UV light. (**A**) *Charmus laneus* Karsch, 1879, adult ♀(IES-628); (**B**) *Charmus sinhagadensis* Tikader & Bastawade, 1983; neotype, adult ♂(BNHS SC 403); (**C**) *Charmus brignolii* Lourenço, 2000; adult ♂(IES-616); (**D**) *Charmus dakshini* sp. nov**.**; holotype, adult ♂(BNHS SC 404), (**E**) *Charmus laneus* Karsch, 1879; adult ♂(Locality 15CN) from Sri Lanka; (**F**) *Charmus saradieli* Kovarik et al. 2016 adult ♂(Locality 18 CO) from Sri Lanka. Scale bars: 2 mm. Remark: an adult female specimen of *Charmus laneus* was photographed due to unavailability of an intact adult male specimen.
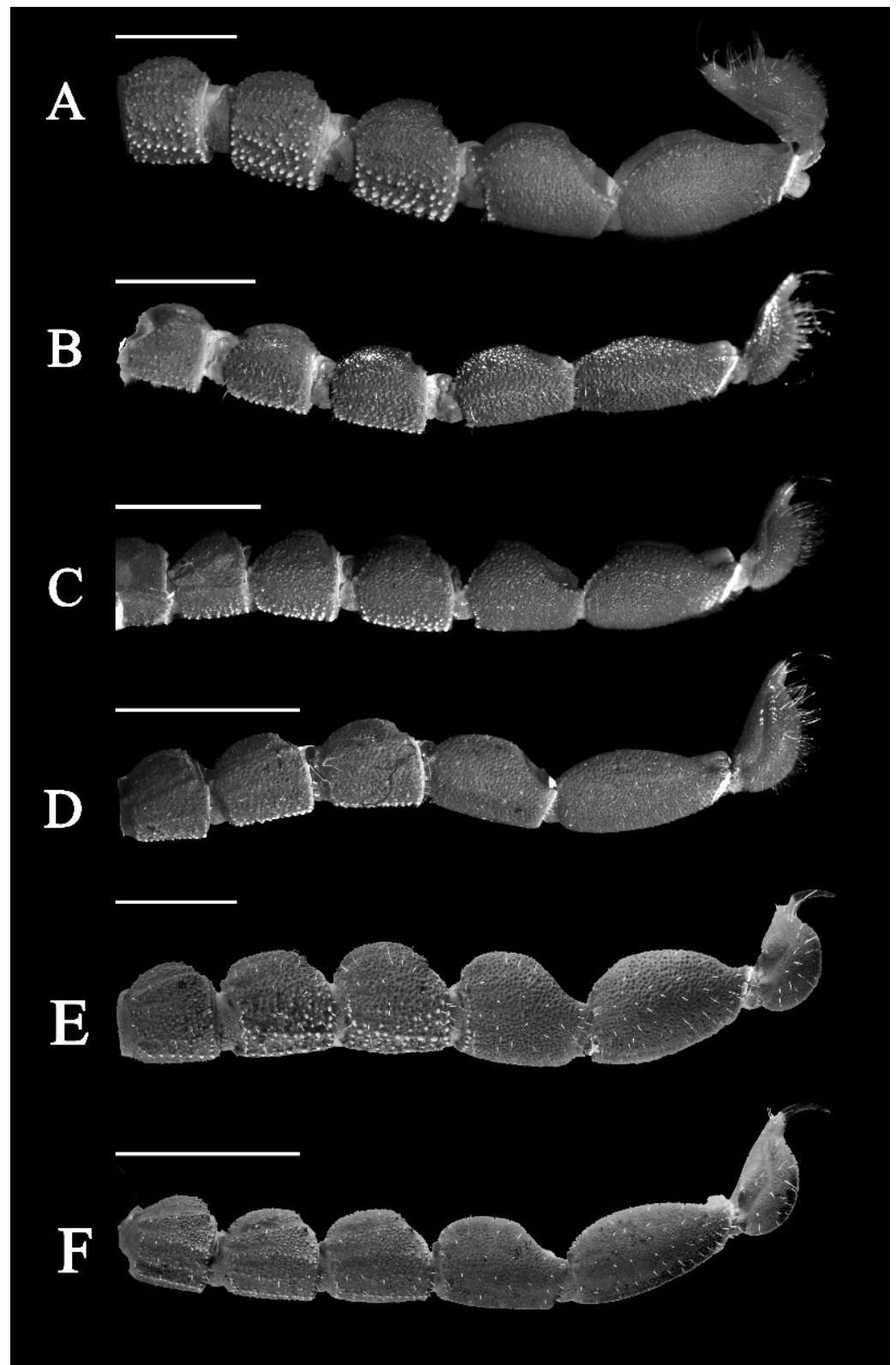
Figure 18. Metasomal segments lateral view under UV light. (**A**) *Charmus laneus* Karsch, 1879, adult ♀(IES-628); (**B**) *Charmus sinhagadensis* Tikader & Bastawade, 1983; neotype, adult ♂(BNHS SC 403); (**C**) *Charmus brignolii* Lourenço, 2000; adult ♂(IES-616); (**D**) *Charmus dakshini* sp. nov.; holotype, adult ♂(BNHS SC 404), (**E**) *Charmus laneus* Karsch, 1879; adult ♂(Locality 15CN) from Sri Lanka; (**F**) *Charmus saradieli* Kovarik et al. 2016 adult ♂(Locality 18 CO) from Sri Lanka. Scale bars: 2 mm. Remark: an adult female specimen of *Charmus laneus* was photographed due to the unavailability of an intact adult male specimen.
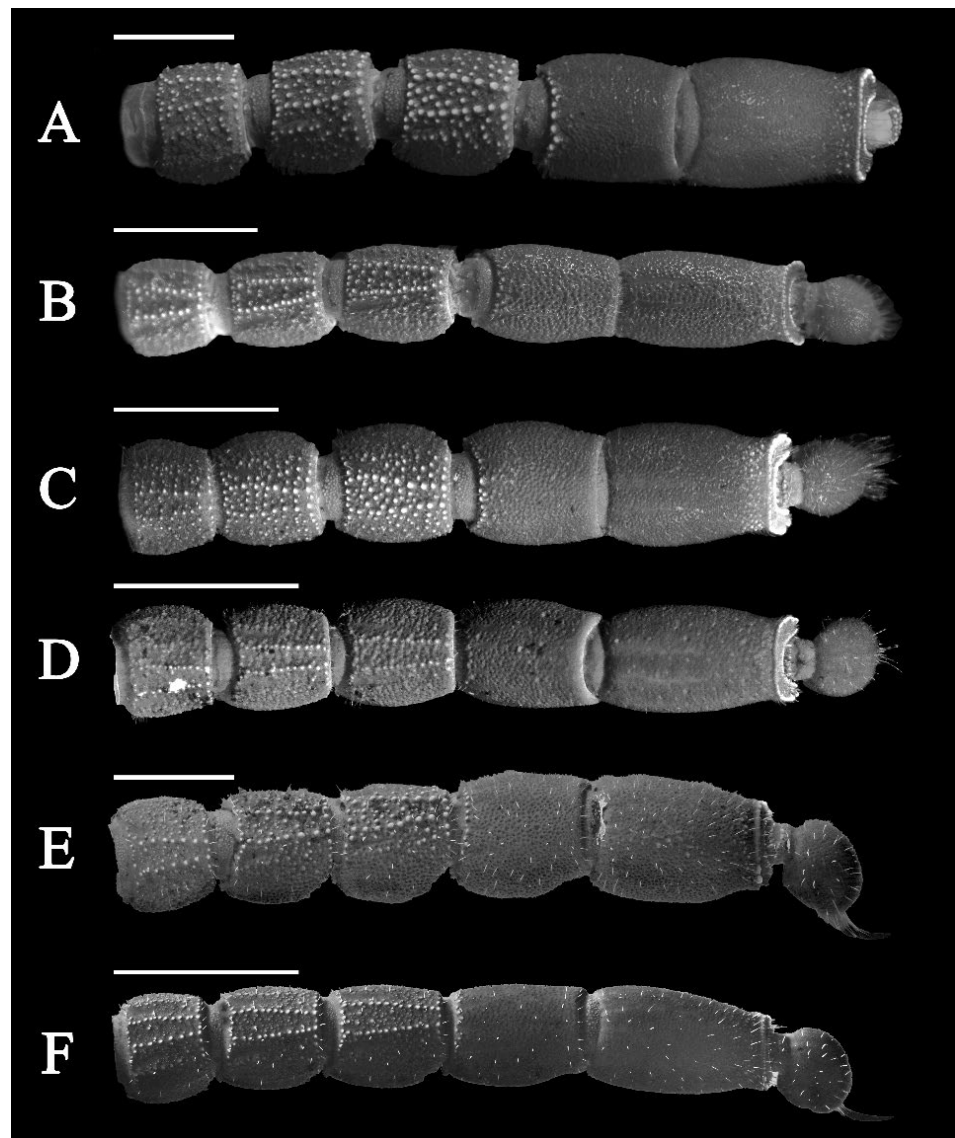
Figure 19. Metasomal segments ventral view under UV light. (**A**) *Charmus laneus* Karsch, 1879, adult ♀(IES-628); (**B**) *Charmus sinhagadensis* Tikader & Bastawade, 1983; neotype, adult ♂(BNHS SC 403); (**C**) *Charmus brignolii* Lourenço, 2000; adult ♂(IES-616); (**D**) *Charmus dakshini* sp. nov.; holotype, adult ♂(BNHS SC 404), (**E**) *Charmus laneus* Karsch, 1879; adult ♂(Locality 15CN) from Sri Lanka; (**F**) *Charmus saradieli* Kovarik et al. 2016 adult ♂(Locality 18 CO) from Sri Lanka. Scale bars: 2 mm. Remark: an adult female specimen of *Charmus laneus* was photographed due to the unavailability of an intact adult male specimen.
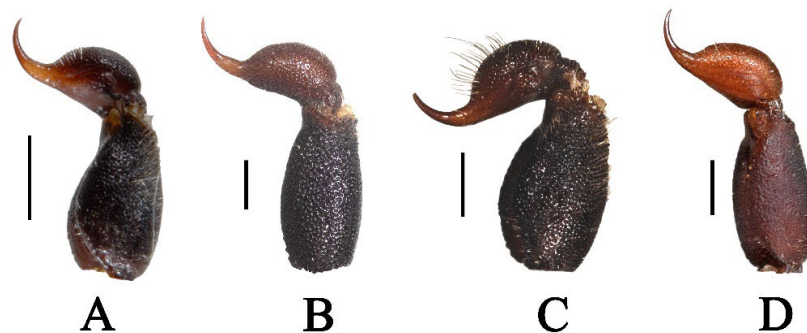
Figure 20. Metasomal segment V and telson lateral view. (**A**) *Charmus laneus*, adult ♂(IES-631); (**B**) *Charmus sinhagadensis*; neotype, adult ♂(BNHS SC 403); (**C**) *Charmus brignolii*; adult ♂(IES-616); (**D**) *Charmus dakshini* sp. nov.; holotype, adult ♂(BNHS SC 404) Scale bars: 1 mm.

4. Results

4.1. Molecular Phylogeny of Charmus Based on Sanger-Sequenced Data (Figure 21 and Figure S1)

The genus *Charmus* is recovered as monophyletic and sister to the clade ((*Parabuthus* + *Karasbergia*) ((*Thaicharmus* + *Buthoscorpio*) (*Grosphus* + *Teruelius*)) in the IQ-TREE analysis, whereas it clusters with *Uroplectes gracilior* in a clade sister to ((*Parabuthus* + *Karasbergia*) ((*Thaicharmus* + *Buthoscorpio*) (*Grosphus* + *Teruelius*))) in the RAxML analysis. *Charmus brignolii* is recovered as the more basal element in *Charmus* and sister to the clade comprising all other species in both analyses. *Charmus sinhagadensis* is recovered as monophyletic and sister to the clade (*C. saradieli* (*C. laneus* + *C. dakshini* sp. nov.)) in both analyses. *Charmus saradieli* is sister to the clade (*C. laneus* + *C. dakshini* sp. nov.) in both analyses. Finally, *Charmus dakshini* sp. nov. is always recovered as the sister species to *C. laneus*.
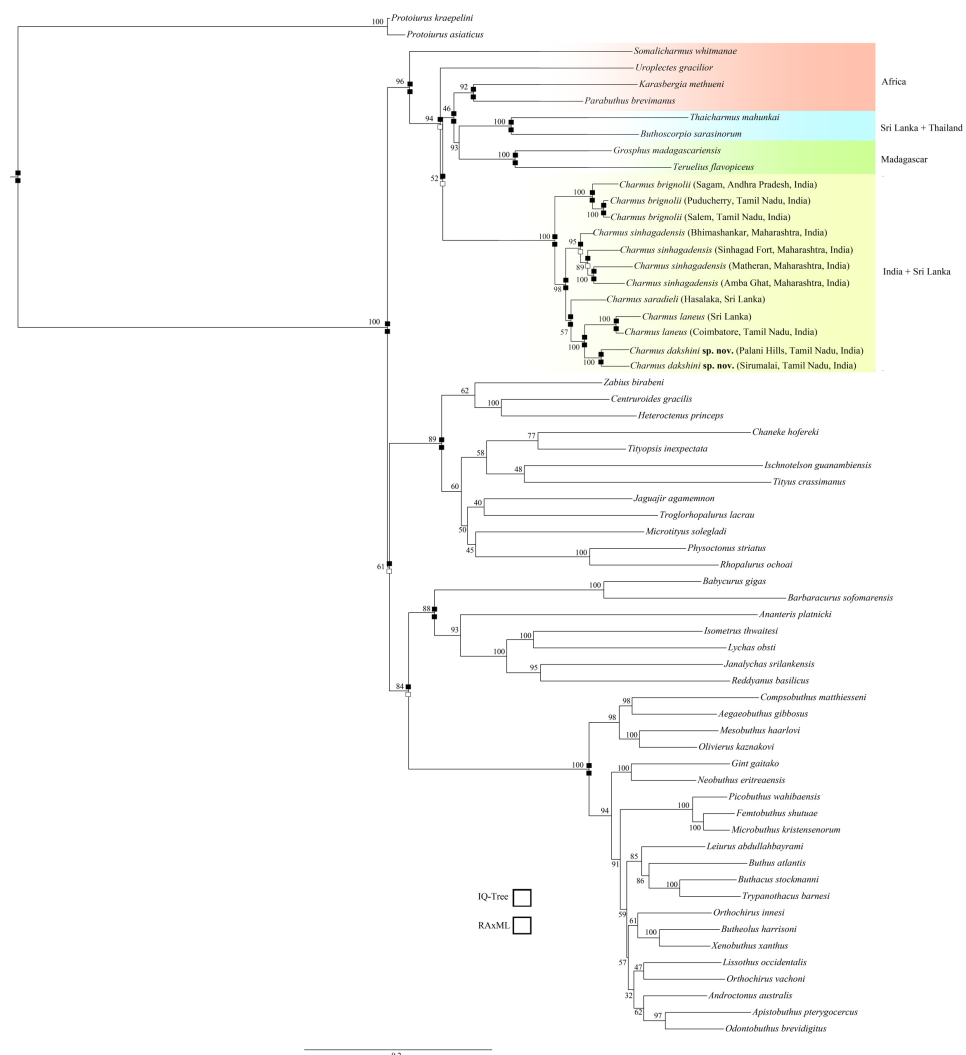
Figure 21. Tree topology based on Maximum Likelihood (ML) analysis of Sanger-sequencing data (IQ-Tree). Values at the nodes are bootstraps for 1000 iterations. Navajo rugs indicate recovery of nodes for IQ Tree and RAxML analysis.

4.2. Comparisons of p-Distance with Closest Related Congeners (Tables S1–S3)

The new species *C. dakshini* sp. nov. is more closely related to *C. laneus* and differs by a raw genetic divergence of 9.4–11.4% and 6.4–7.1% on the COI and 16S genes, respectively. The new species is separated from *C. brignolii* by a raw genetic divergence of 10.1–12.4% and 9.4–10.7% on the COI and 16S genes, respectively. *Charmus brignolii* differs from *C.*

laneus by a high raw genetic divergence of 10.3–13.6% and 9.4–10.7% on the COI and 16S genes, respectively. Specimens of *C. laneus* collected from Coimbatore, Tamil Nadu differ by a raw genetic divergence of 6.7% and 1.5% from *C. laneus* samples collected at the type locality on the COI and 16S genes, respectively. Based on the COI gene, the population of *C. dakshini* sp. nov. from Palani Hills, Tamil Nadu differs by a raw genetic divergence of 6.7% from the ones collected at the type locality. The populations of *C. brignolii* from Salem (Tamil Nadu), and Sangam (Andhra Pradesh) differ from *C. brignolii* collected at the type locality by a raw genetic divergence of 1.6% and 6.2% on the COI gene. The populations of *C. sinhagadensis* from Matheran, Amba Ghat, and Bhimashankar in Maharashtra show raw genetic divergences from *C. sinhagadensis* collected at the type locality of 8.6%, 8.4%, and 8.3%, respectively, on the COI gene. Additionally, the Bhimashankar population exhibits a divergence of 4.8% on the 16S gene from the population at the type locality. Based on the 28S gene data, *C. laneus* from Sri Lanka shows no genetic divergence from *C. laneus* collected from Coimbatore. *Charmus saradieli* differs from *C. laneus* by a raw genetic divergence of 0.6%. The populations of *C. brignolii* from Puducherry and Sangam (Andhra Pradesh) show an intraspecific divergence of 0.2% and differ from *C. laneus* by a raw genetic divergence of 0.6–0.8%. The populations of *C. sinhagadensis* from Sinhagad Fort, Bhimashankar and Amba Ghat show no intraspecific genetic divergence based on the 28S gene data. *Charmus sinhagadensis* shows a raw interspecific genetic divergence of 0.8–1.1% with the populations of *C. brignolii* and 0.2% with *C. laneus*.

4.3. Molecular Phylogenetics Based on the UCE Data (Figure 22)

Analyses of the various matrices recovered the same topology. The genus *Charmus* is recovered to be monophyletic and the sister group of *Buthoscorpio* Werner, 1936. The clade (*Charmus* + *Buthoscorpio*) is observed to be sister to *Grosphus* Simon, 1880. The clade (*Grosphus* (*Charmus* + *Buthoscorpio*)) is found to be a sister to *Parabuthus* Pocock, 1890 and (*Parabuthus* (*Grosphus* (*Charmus* + *Buthoscorpio*)) is itself sister to *Uroplectes* Peters, 1861. *Charmus sinhagadensis* from Amba Ghat and Bhimashankar (Maharashtra) is recovered to be a sister to *Charmus dakshini* sp. nov. *Charmus brignolii* is recovered to be a sister to the clade (*C. sinhagadensis* + *C. dakshini* sp. nov.).
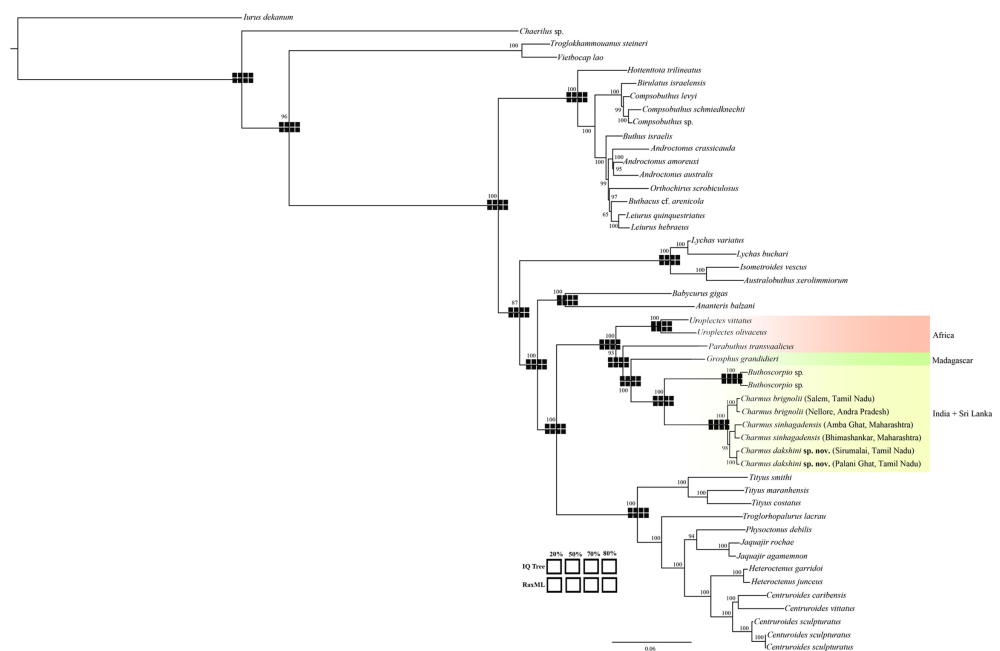

Figure 22. Tree topology based on Maximum likelihood (ML) analysis of the UCE data. Navajo rugs indicate the recovery of nodes given the different occupancy matrices (20%, 50%, 70% and 80%).

5. Discussion

5.1. Congruence Between Morphology, Genetic Divergence, Phylogeny and Geography

Based on the genetic divergence computed for COI and 16S genes, the intraspecific variation is determined to be 8.6% or below for the COI gene and 4.8% or below for the 16S gene. Interestingly, the intraspecific variations reported for *C. sinhagadensis* samples (8.3–8.6% on COI and 4.8% on 16S) are much higher than those reported for *C. brignolii* (1.6–6.2% on COI), *C. dakshini* sp. nov. (6.7% on COI) and *C. laneus* (6.7% on COI and 1.5% on 16S). On the other hand, interspecific genetic divergence is at least 9.4% and 6.4% for COI and 16S, respectively. We hereby consider that a sample exhibiting a genetic divergence of 9.4% or more on the COI gene and/or a genetic divergence of 6.4% or more on the 16S gene, is to be considered as a distinct species, provided its distinctness holds against other lines of evidence.

The Sanger phylogeny generated here is congruent with the different morpho-species defined and the different genetic divergences calculated (inter- and intraspecific). Moreover, the geographical structure of the data is also in agreement with the phylogeny. *Charmus* is divided into three clades with distinct non-overlapping distribution ranges, i.e., the *C. brignolii* clade occurring in the plains of south-eastern India, the *C. sinhagandensis* clade occurring in the northern Western Ghats and the *C. laneus* clade (*C. dakshini* sp. nov., *C. laneus*, *C. saradieli*) occurring in the southern Western Ghats and Sri Lanka (Figure 23).
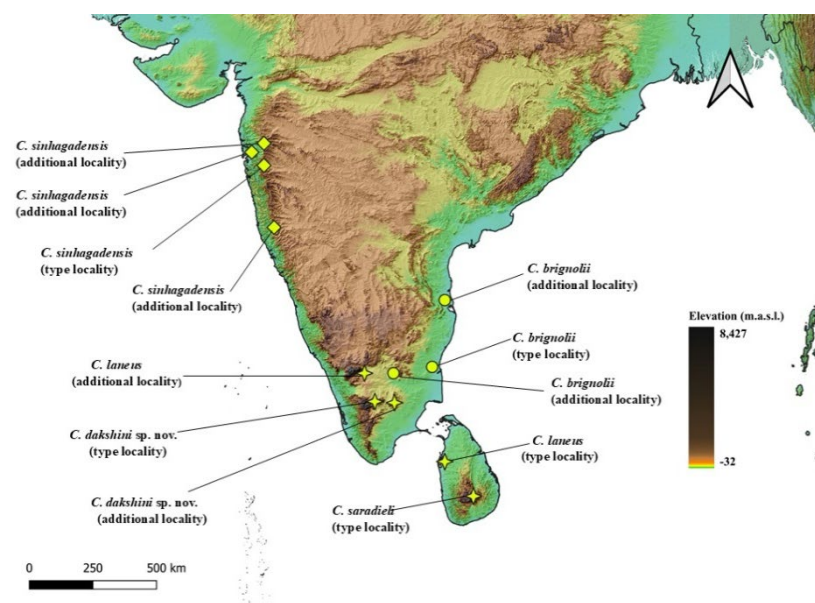
Figure 23. Distribution of *Charmus* Karsch, 1879 in India and Sri Lanka with elevation data. The diamonds represent the *C. sinhagadensis* clade, circles represent the *C. brignolii* clade and the stars represent the *C. laneus* clade.

The alpha taxonomic study of the genus is strongly reinforced here by the analysis of genetic data, both comparatively and phylogenetically, as well as by the geographical pattern observed. The congruence between results from these various analyses allows us to propose a solid systematics assessment of *Charmus*.

5.2. Morphological Difference Between Lowland and Highland Species

Charmus brignolii and *C. laneus* are confined to the lowland grassland patches of Tamil Nadu and Andhra Pradesh (84–388 m). *C. dakshini* sp. nov. is found at comparatively higher elevations (813–1600 m), inhabiting the semi-evergreen forests of Palani Hills and Sirumalai. Similarly, *C. sinhagadensis* is also found at high elevations in the moist deciduous forests

of the northern Western Ghats (455–1315 m). A feature worth mentioning is the reduced carination and overall granulation on metasomal segments observed in these two highland species (>700 m a.s.l.) when compared to the lowland species. Moreover, while highland species are bound to moist habitats, lowland species occur in much drier ecosystems.

We here hypothesize that the different degrees of cuticular carination and granulation observed in *Charmus* species are directly linked to the air temperatures and humidity levels. In arthropods, cuticular structures and patterning are known to influence the surface interaction with water [71]. For instance, on textured surfaces, water droplets will be suspended on top of the observed structures, creating a three-phase liquid–air–solid interface known as the Cassie–Baxter model [72,73]. In this model, an air pocket trapped between the droplets and the structured surface prevents the surface from getting wet. This interface will then have a cooling effect on the underlying surface. Moreover, dropwise condensation increases with the roughness of the surface, resulting in more heat transfer and cooling. Conversely, smooth surfaces are not able to accumulate the water as much as textured surfaces, and thus will not generate the same cooling effect. The textured cuticle of the lowland species may help them cope with low levels of air humidity and high temperatures—environmental constraints that highland species do not have.

5.3. Topological Differences Between Phylogenies

The genus *Charmus* is consistently grouped with South African and Malagasy taxa in both UCE and Sanger analyses, which is consistent with the Gondwana break-up history [74,75]. The UCE tree consistently reveals stable phylogenetic relationships with strong nodal supports across various analyses of several occupancy matrices. The following topological sequence is retrieved in all analyses: (*Uroplectes* (*Parabuthus* (*Grosphus* + (*Buthoscorpio* + *Charmus*)))). However, analyses of Sanger data with IQ-TREE and RAxML yield slightly different topologies with some weakly supported nodes: (*Uroplectes* ((*Parabuthus* + *Karasbergia*) (*Charmus* ((*Thaicharmus* + *Buthoscorpio*) (*Grosphus* + *Teruelius*))))) in the RAxML analysis, ((*Uroplectes* + *Charmus*) ((*Parabuthus* + *Karasbergia*) ((*Thaicharmus* + *Buthoscorpio*) (*Grosphus* + *Teruelius*)))). The assumption that the UCEs are more suitable for resolving higher-level relationships is confirmed here. The Sanger phylogenies do not provide a consensus topology, and the branch supports remain insufficient to consider it reliable. On the other hand, the topology computed by analyses of the UCE dataset remains constant and well-supported.

Whereas *Charmus* is sister to *Buthoscorpio* in UCE analysis, it is retrieved as sister to a clade comprising *Buthoscorpio*, *Thaicharmus*, *Grosphus*, *Teruelius*, *Karasbergia* and *Parabuthus* in the IQ-TREE analysis of Sanger data and as sister to *Uroplectes* in the RAxML analysis of Sanger data, albeit with low branch support. The morphology and geographical distribution of *Buthoscorpio* and *Thaicharmus* suggest that they are more closely related to *Charmus* than to *Grosphus*/*Teruelius*. The UCE topology is congruent with this assumption and is considered as more reliable than those generated with Sanger data. However, this cannot be presently unambiguously proven because a sample of *Thaicharmus* is currently missing in the UCE dataset. Therefore, additional UCE phylogenetic analyses with an updated dataset need to be conducted before the status of *Charmus* within the family Buthidae is further clarified.

5.4. Biogeographic Considerations

The Southern Western Ghats (SWG) and the Central Highlands of Sri Lanka acted as refugia for many groups of the Indian wet evergreen fauna and flora during the KT Mass Extinction [76–79]. It is expected from this pattern that the lineages occurring in the SWG are ancient and more diverse, whereas those occurring in the northern and central Western Ghats (NWG and CWG) are less speciose, relatively younger and phylogenetically

nested [80]. However, the phylogeny of *Charmus* partially contradicts this biogeographic pattern. The basal species *C. brignolii* is not present in the Western Ghats but rather occurs on the southeastern plains. Furthermore, *C. sinhagadensis* seems to be restricted to the NWG whereas its sister group (*C. saradieli* (*C. laneus* + *C. dakshini* sp. nov.)) is probably endemic to the SWG and Sri Lanka. Interestingly, no *Charmus* species are currently known from the CWG suggesting that either *Charmus* is present in the area but has not been collected yet or that, contrary to the NWG and SWG, the CWG were not sufficiently stable environmentally to ensure the survival of *Charmus* during range contractions. This interesting biogeographic pattern needs to be tested separately using dated phylogenies and dispersal-vicariance analyses.

References

1. Perera, S.J.; Suranjanfernando, R.H.S. Physiography, Climate, and Historical Biogeography of Sri Lanka in Making a Biodiversity Hotspot. In *Biodiversity Hotspots of the Western Ghats and Sri Lanka*; Apple Academic Press: Palm Bay, FL, USA, 2022; pp. 405–445.
2. Dissanayake, C.B.; Chandrajith, R. Sri Lanka–Madagascar Gondwana Linkage: Evidence for a Pan-African Mineral Belt. *J. Geol.* **1999**, *107*, 223–235. [CrossRef]
3. Deepak, V.; Karanth, P. Aridification Driven Diversification of Fan-Throated Lizards from the Indian Subcontinent. *Mol. Phylogenet. Evol.* **2018**, *120*, 53–62. [CrossRef] [PubMed]
4. Gorin, V.A.; Solovyeva, E.N.; Hasan, M.; Okamiya, H.; Karunarathna, D.M.S.S.; Pawangkhanant, P.; de Silva, A.; Juthong, W.; Milto, K.D.; Nguyen, L.T.; et al. A little frog leaps a long way: Compounded colonizations of the Indian Subcontinent discovered in the tiny Oriental frog genus Microhyla (Amphibia: Microhylidae). *PeerJ* **2020**, *8*, e9411. [CrossRef] [PubMed]

5. Prendini, L.; Weygoldt, P.; Wheeler, W.C. Systematics of the *Damon variegatus* group of African whip spiders (Chelicerata: Amblypygi): Evidence from behavior, morphology, and DNA. *Org. Divers. Evol.* **2005**, *5*, 203–236. [CrossRef]

6. Seiter, M.; Lerma, A.; Král, J.; Sember, A.; Divišová, K.; Palacios-Vargas, J.; Colmenares, P.A.; Loria, S.F.; Prendini, L. Cryptic diversity in the whip spider genus *Paraphrynus* (Amblypygi: Phrynidae): Integrating morphology, karyotype, and DNA. *Arthropod Syst. Phylogeny* **2020**, *78*, 265–285.

7. Schramm, F.D.; Valdez-Mondragón, A.; Prendini, L. Volcanism and palaeoclimate change drive diversification of the world's largest whip spider (Amblypygi). *Mol. Ecol.* **2021**, *12*, 2872–2890. [CrossRef]

8. Karsch, F. Skorpionologische Beiträge I. und II. *Mitt. Münch. Entomol. Ver.* **1879**, *3*, 6–22, 97–136.

9. Hirst, S. Description of a new Indian Scorpion (*Charmus indicus* sp. n.). *Ann. Mag. Nat. Hist.* **1915**, *15*, 224–225. [CrossRef]

10. Sreenivasa-Reddy, R.P. Contribution à la connaissance des Scorpions de l'Inde. I. *Charmus indicus* Hirst, 1915 (Fam. Buthidae). *Bull. Mus. Natl. Hist.* **1966**, *38*, 247–256.

11. Tikader, B.K.; Bastawade, D.B. *The Fauna of India*; Zoological Survey of India: Calcutta, India, 1983; Volume 3, pp. 146–152.

12. Lourenço, W.R. Taxonomic considerations about the genus *Charmus* Karsch, 1879 with description of a new species to India (Scorpiones: Buthidae). *Mem. Soc. Entomol.* **2000**, *78*, 295–303.

13. Lourenço, W.R. Further taxonomic considerations about the genus *Charmus* Karsch, 1879 (Scorpiones, Buthidae), with the description of a new species from Sri Lanka. *Entomol. Mitt. Zool. Mus. Hamb.* **2002**, *14*, 17–25.

14. Kovarik, F.; Lowe, G.; Ranawana, K.B.; Hoferek, D.; Jayarathne, V.A.S.; Pliskova, J. Scorpions of Sri Lanka (Arachnida, Scorpiones: Buthidae, Chaerilidae, Scorpionidae) with Description of Four New Species of the Genera *Charmus* Karsch, 1879 and *Reddyanus* Vachon, 1972, stat. n. *Euscorpius* **2016**, *220*, 1–133. [CrossRef]

15. International Commission on Zoological Nomenclature (ICZN). *International Code of Zoological Nomenclature*; Online Edition; International Commission on Zoological Nomenclature (ICZN): Singapore, 2000; Available online: https://www.iczn.org/the-code/the-international-code-of-zoological-nomenclature/the-code-online/ (accessed on 7 December 2024).

16. Wong, E.S.; Dahlem, G.A.; Stamper, T.I.; DeBry, R.W. Discordance between Morphological Species Identification and mtDNA Phylogeny in the Flesh Fly Genus *Ravinia* (Diptera: Sarcophagidae). *Invertebr. Syst.* **2015**, *29*, 1–11. [CrossRef]

17. Andriaholinirina, N.; Fausser, J.L.; Roos, C.; Zinner, D.; Thalmann, U.; Rabarivola, C.; Ravoarimanana, I.; Ganzhorn, J.U.; Meier, B.; Hilgartner, R.; et al. Molecular Phylogeny and Taxonomic Revision of the Sportive Lemurs (Lepilemur, Primates). *BMC Evol. Biol.* **2006**, *6*, 1–13. [CrossRef]

18. Cook, L.G.; Edwards, R.D.; Crisp, M.D.; Hardy, N.B. Need Morphology Always Be Required for New Species Descriptions? *Invertebr. Syst.* **2010**, *24*, 322–326. [CrossRef]

19. Gullan, P.J.; Downie, D.A.; Steffan, S.A. A New Pest Species of the Mealybug Genus *Ferrisia* Fullaway (Hemiptera: Pseudococcidae) from the United States. *Ann. Entomol. Soc. Am.* **2003**, *96*, 723–737. [CrossRef]

20. Sharma, P.K.; Fernández, R.M.N.; Esposito, L.A.; González-Santillán, E.; Monod, L. Phylogenomic Resolution of Scorpions Reveals Multilevel Discordance with Morphological Phylogenetic Signal. *Proc. R. Soc. B Biol. Sci.* **2015**, *282*, 20142953. [CrossRef]

21. Santibáñez-López, C.E.; Ojanguren-Affilastro, A.A.; Sharma, P.P. Another One Bites the Dust: Taxonomic Sampling of a Key Genus in Phylogenomic Datasets Reveals More Non-Monophyletic Groups in Traditional Scorpion Classification. *Invertebr. Syst.* **2020**, *34*, 133–143. [CrossRef]

22. Štundlová, J.; Šťáhlavský, F.; Opatova, V.; Stundl, J.; Kovařík, F.; Dolejš, P.; Šmíd, J. Molecular Data Do Not Support the Traditional Morphology-Based Groupings in the Scorpion Family Buthidae (Arachnida: Scorpiones). *Mol. Phylogenet. Evol.* **2022**, *173*, 107511. [CrossRef]

23. Svenson, G.J.; Whiting, M.F. Reconstructing the origins of praying mantises (Dictyoptera: Mantodea): The roles of Gondwanan vicariance and morphological convergence. *Cladistics* **2009**, *25*, 468–514. [CrossRef]

24. Hendrixson, E.; Bond, J.E. Evaluating the efficacy of continuous quantitative characters for reconstructing the phylogeny of a morphologically homogeneous spider taxon (Araneae, Mygalomorphae, Antrodiaetidae, Antrodiaetus). *Mol. Phylogenet. Evol.* **2009**, *53*, 300–313. [CrossRef] [PubMed]

25. Ortiz, D.; Francke, O.F.; Bond, J.E. A tangle of forms and phylogeny: Extensive morphological homoplasy and molecular clock heterogeneity in *Bonnetina* and related tarantulas. *Mol. Phylogenet. Evol.* **2018**, *127*, 55–73. [CrossRef] [PubMed]

26. Opatova, V.; Hamilton, C.A.; Hedin, M.; Montes De Oca, L.; Král, J.; Bond, J.E. Phylogenetic systematics and evolution of the spider infraorder Mygalomorphae using genomic scale data. *Syst. Biol.* **2020**, *69*, 671707. [CrossRef] [PubMed]

27. Masonick, P.K.; Knyshov, A.; Gordon, E.R.L.; Forero, D.; Hwang, W.S.; Hoey-Chamberlain, R.; Bush, T.; Castillo, S.; Hernandez, M.; Ramirez, J.; et al. A revised classification of the assassin bugs (Hemiptera: Heteroptera: Reduviidae) based on combined analysis of phylogenomic and morphological data. *Syst. Entomol.* **2025**, *50*, 102–138. [CrossRef]

28. Sharma, P.P.; Kaluziak, S.T.; Pérez-Porro, A.R.; González, V.L.; Hormiga, G.; Wheeler, W.C.; Giribet, G. Phylogenomic interrogation of Arachnida reveals systemic conflicts in phylogenetic signal. *Mol. Biol. Evol.* **2014**, *31*, 2963–2984. [CrossRef]

29. Agnarsson, I.; Coddington, J.A.; Kuntner, M. Systematics: Progress in the study of spider diversity and evolution. In *Spider Research in the 21st Century: Trends and Perspectives*; Penney, D., Ed.; Siri Scientific Press: Greater Manchester, UK, 2013; pp. 58–111.

30. Bond, J.E.; Garrison, N.L.; Hamilton, C.A.; Godwin, R.L.; Hedin, M.; Agnarsson, I. Phylogenomics resolves a spider backbone phylogeny and rejects a prevailing paradigm for orb web evolution. *Curr. Biol.* **2014**, *24*, 1765–1771. [CrossRef] [PubMed]

31. Fernández, R.; Hormiga, G.; Giribet, G. Phylogenomic analysis of spiders reveals nonmonophyly of orb weavers. *Curr. Biol.* **2014**, *24*, 1772–1777. [CrossRef]

32. Godwin, R.L.; Opatova, V.; Garrison, N.L.; Hamilton, C.A.; Bond, J.E. Phylogeny of a cosmopolitan family of morphologically conserved trapdoor spiders (Mygalomorphae, Ctenizidae) using Anchored Hybrid Enrichment, with a description of the family Halonoproctidae Pocock 1901. *Mol. Phylogenet. Evol.* **2018**, *126*, 303–313. [CrossRef]

33. Hedin, M.; Derkarabetian, S.; Ramírez, M.J.; Vink, C.; Bond, J.E. Phylogenomic reclassification of the world's most venomous spiders (Mygalomorphae, Atracinae), with implications for venom evolution. *Sci. Rep.* **2018**, *8*, 1636. [CrossRef]

34. Wood, H.M.; González, V.L.; Lloyd, M.; Coddington, J.; Scharff, N. Next-generation Museum genomics: Phylogenetic relationships among palpimanoid spiders using sequence capture techniques (Araneae: Palpimanoidea). *Mol. Phylogenet. Evol.* **2018**, *127*, 907–918. [CrossRef]

35. Kulkarni, S.; Kallal, B.; Wood, H.; Dimitrov, D.; Giribet, G.; Hormiga, G. Interrogating genomic-scale data to resolve recalcitrant nodes in the spider tree of life. *Mol. Biol. Evol.* **2020**, *38*, 891–903. [CrossRef] [PubMed]

36. Faircloth, B.C.; McCormack, J.E.; Crawford, N.G.; Harvey, M.G.; Brumfield, R.T.; Glenn, T.C. Ultraconserved elements anchor thousands of genetic markers spanning multiple evolutionary timescales. *Syst. Biol.* **2012**, *61*, 717–726. [CrossRef] [PubMed]

37. Vachon, M. Études des Caractères Utilisés pour Classer les Familles et les Genres de Scorpions (Arachnides). 1. La Trichobothriotaxie en Arachnologie. Sigles Trichobothriaux et Types de Trichobothriotaxie chez les Scorpions. *Bull. Mus. Natl. Hist. Nat.* **1974**, *104*, 857–958.

38. Francke, O.F. Scorpions of the Genus Diplocentrus from Oaxaca, Mexico (Scorpionida, Diplocentridae). *J. Arachnol.* **1977**, *4*, 145–200.

39. González-Santillán, E.; Prendini, L. Redefinition and Generic Revision of the North American Vaejovid Scorpion Subfamily Syntropinae Kraepelin, 1905, with Descriptions of Six New Genera. *Bull. Am. Mus. Nat. Hist.* **2013**, *382*, 1–71. [CrossRef]

40. Hjelle, J.T. Anatomy and morphology. In *The Biology of Scorpions*; Polis, G.A., Cloudsley-Thompson, J., Eds.; Stanford University Press: Stanford, CA, USA, 1990; pp. 9–63.

41. Loria, S.F.; Prendini, L. Homology of the Lateral Eyes of Scorpiones: A Six-Ocellus Model. *PLoS ONE* **2014**, *9*, 1–30. [CrossRef]

42. Volschenk, E.S. A New Technique for Examining Surface Morphosculpture of Scorpions. *J. Arachnol.* **2005**, *33*, 820–825. [CrossRef]

43. Stahnke, H.L. Scorpion Nomenclature and Mensuration. *Entomol. News* **1970**, *81*, 297–316.

44. Starrett, J.; Derkarabetian, S.; Hedin, M.; Bryson, R.W., Jr.; McCormack, J.E.; Faircloth, B.C. High phylogenetic utility of an ultraconserved element probe set designed for Arachnida. *Mol. Ecol. Resour.* **2017**, *17*, 812–823. [CrossRef]

45. Santibáñez-López, C.E.; Aharon, S.; Ballesteros, J.A.; Gainett, G.; Baker, C.M.; González-Santillán, E.; Harvey, M.S.; Hassan, M.K.; Abu-Almaaty, A.H.; Aldeyarbi, S.M.; et al. Phylogenomics of scorpions reveal a co-diversification of scorpion mammalian predators and mammal-specific sodium channel toxins. *Syst. Biol.* **2022**, *71*, 1281–1289. [CrossRef]

46. Sulakhe, S.; Deshpande, S.; Gowande, G.; Dandekar, N.; Ketkar, M. Arboreal Gems: Resurrection of *Isometrus sankeriensis* Tikader & Bastawade, 1983 and Descriptions of Two New Species of *Isometrus* Ehrenberg, 1828 (Scorpiones: Buthidae) from the Western Ghats, India. *Eur. J. Taxon.* **2022**, *811*, 1–50. [CrossRef]

47. Folmer, O.; Black, M.; Hoeh, W.; Lutz, R.; Vrijenhoek, R. DNA primers for amplification of mitochondrial cytochrome c oxidase subunit I from diverse metazoan invertebrates. *Mol. Mar. Biol. Biotechnol.* **1994**, *3*, 294–299. [CrossRef] [PubMed]

48. Simon, C.; Frati, F.; Beckenbach, A.; Crespi, B.; Liu, H.; Flook, P. Evolution, weighting, and phylogenetic utility of mitochondrial gene sequences and a compilation of conserved polymerase chain reaction primers. *Ann. Entomol. Soc. Am.* **1994**, *87*, 651–701. [CrossRef]

49. Giribet, G.; Carranza, S.; Baguñà, J.; Riutort, M.; Ribera, C. First molecular evidence for the existence of a *Tardigrada + Arthropoda* clade. *Mol. Biol. Evol.* **1996**, *13*, 76–84. [CrossRef]

50. Barrett, R.D.H.; Hebert, P.D.N. Identifying spiders through DNA barcodes. *Can. J. Zool.* **2005**, *83*, 481–491. [CrossRef]

51. Benson, D.A.; Cavanaugh, M.; Clark, K.; Karsch-Mizrachi, I.; Lipman, D.J.; Ostell, J.; Sayers, E.W. GenBank. *Nucleic Acids Res.* **2017**, *45*, D37–D42. [CrossRef]

52. Kumar, S.; Stecher, G.; Tamura, K. MEGA7: Molecular Evolutionary Genetics Analysis Version 7.0 for Bigger Datasets. *Mol. Biol. Evol.* **2016**, *33*, 1870–1874. [CrossRef]

53. Edgar, R.C. MUSCLE: Multiple Sequence Alignment with High Accuracy and High Throughput. *Nucleic Acids Res.* **2004**, *32*, 1792–1797. [CrossRef]

54. Nguyen, L.T.; Schmidt, H.A.; Von Haeseler, A.; Minh, B.Q. IQ-TREE: A Fast and Effective Stochastic Algorithm for Estimating Maximum-Likelihood Phylogenies. *Mol. Biol. Evol.* **2015**, *32*, 268–274. [CrossRef]

55. Edler, D.; Klein, J.; Antonelli, A.; Silvestro, D. raxmlGUI 2.0: A graphical interface and toolkit for phylogenetic analyses using RAxML. *Methods Ecol. Evol.* **2021**, *12*, 373–377. [CrossRef]

56.   Kalyaanamoorthy, S.; Minh, B.Q.; Wong, T.K.; Von Haeseler, A.; Jermiin, L.S. ModelFinder: Fast Model Selection for Accurate Phylogenetic Estimates. *Nat. Methods* **2017**, *14*, 587–589. [CrossRef] [PubMed]

57.   Hoang, D.T.; Chernomor, O.; Von Haeseler, A.; Minh, B.Q.; Vinh, L.S. UFBoot2: Improving the Ultrafast Bootstrap Approximation. *Mol. Biol. Evol.* **2018**, *35*, 518–522. [CrossRef] [PubMed]

58.   Minh, B.Q.; Schmidt, H.A.; Chernomor, O.; Schrempf, D.; Woodhams, M.D.; Von Haeseler, A.; Lanfear, R. IQ-TREE 2: New Models and Efficient Methods for Phylogenetic Inference in the Genomic Era. *Mol. Biol. Evol.* **2020**, *37*, 1530–1534. [CrossRef] [PubMed]

59.   Lanfear, R.; Calcott, B.; Ho, S.Y.W.; Guindon, S. PartitionFinder: Combined Selection of Partitioning Schemes and Substitution Models for Phylogenetic Analyses. *Mol. Biol. Evol.* **2012**, *29*, 1695–1701. [CrossRef]

60.   Schwarz, G. Estimating the Dimension of a Model. *Ann. Stat.* **1978**, *6*, 461–464. [CrossRef]

61.   Suchan, T.; Pitteloud, C.; Gerasimova, N.S.; Kostikova, A.; Schmid, S.; Arrigo, N.; Pajkovic, M.; Ronikier, M.; Alvarez, N. Hybridization Capture Using RAD Probes (hyRAD), a New Tool for Performing Genomic Analyses on Collection Specimens. *PLoS ONE* **2016**, *11*, e0151651. [CrossRef]

62.   Meyer, M.; Kircher, M. Illumina Sequencing Library Preparation for Highly Multiplexed Target Capture and Sequencing. *Cold Spring Harb. Protoc.* **2010**, *2010*, pdb-prot5448. [CrossRef]

63.   Faircloth, B.C. Identifying conserved genomic elements and designing universal bait sets to enrich them. *Methods Ecol. Evol.* **2017**, *8*, 1103–1112. [CrossRef]

64.   Grabherr, M.G.; Haas, B.J.; Yassour, M.; Levin, J.Z.; Thompson, D.A.; Amit, I.; Adiconis, X. Trinity: Reconstructing a Full-Length Transcriptome Without a Genome from RNA-Seq Data. *Nat. Biotechnol.* **2011**, *29*, 644. [CrossRef]

65.   Bankevich, A.; Nurk, S.; Antipov, D.; Gurevich, A.A.; Dvorkin, M.; Kulikov, A.S.; Lesin, V.M.; Nikolenko, S.I.; Pham, S.; Prjibelski, A.D.; et al. SPAdes: A new genome assembly algorithm and its applications to single-cell sequencing. *J. Comput. Biol.* **2012**, *19*, 455–477. [CrossRef]

66.   Faircloth, B.C. PHYLUCE is a software package for the analysis of conserved genomic loci. *Bioinformatics* **2016**, *32*, 786–788. [CrossRef] [PubMed]

67.   Katoh, K.; Standley, D.M. MAFFT Multiple Sequence Alignment Software Version 7: Improvements in Performance and Usability. *Mol. Biol. Evol.* **2013**, *30*, 772–780. [CrossRef]

68.   Castresana, J. Selection of Conserved Blocks from Multiple Alignments for Their Use in Phylogenetic Analysis. *Mol. Biol. Evol.* **2000**, *17*, 540–552. [CrossRef] [PubMed]

69.   Talavera, G.; Casteresana, J. Improvement of phylogenies after removing divergent and ambiguously aligned blocks from protein sequence alignments. *Syst. Biol.* **2007**, *56*, 564–577. [CrossRef] [PubMed]

70.   Stamatakis, A.; Hoover, P.; Rougemont, J. A Rapid Bootstrap Algorithm for the RAxML Web Servers. *Syst. Biol.* **2008**, *57*, 758–771. [CrossRef]

71.   Bello, E.; Chen, Y.; Alleyne, M. Staying Dry and Clean: An Insect's Guide to Hydrophobicity. *Insects* **2023**, *14*, 42. [CrossRef]

72.   Wenzel, R.N. Resistance of Solid Surfaces to Wetting by Water. *Ind. Eng. Chem.* **1936**, *28*, 988–994. [CrossRef]

73.   Cassie, A.B.D.; Baxter, S. Wettability of Porous Surfaces. *Trans. Faraday Soc.* **1944**, *40*, 546–551. [CrossRef]

74.   Mani, M.S. (Ed.) *Ecology and Biogeography in India*, 3rd ed.; Dr. W. Junk, B.V., Publishers: The Hague, The Netherlands, 1974; pp. 154–196.

75.   Aitchison, J.C.; Ali, J.R.; Davis, A.M. When and where did India and Asia collide? *J. Geophys. Res. Solid Earth* **2007**, *112*, B05423. [CrossRef]

76.   Conti, E.; Eriksson, T.; Schönenberger, J.; Sytsma, K.J.; Baum, D.A. Early Tertiary Out-of-India dispersal of Crypteroniaceae: Evidence from phylogeny and molecular dating. *Evolution* **2002**, *56*, 1931–1942.

77.   Bossuyt, F.; Brown, R.M.; Hillis, D.M.; Cannatella, D.C.; Milinkovitch, M.C. Phylogeny and biogeography of a cosmopolitan frog radiation: Late Cretaceous diversification resulted in continent-scale endemism in the family Ranidae. *Syst. Biol.* **2006**, *55*, 579–594. [CrossRef] [PubMed]

78.   Joshi, J.; Karanth, P. Did southern Western Ghats of peninsular India serve as refugia for its endemic biota during the Cretaceous volcanism? *Ecol. Evol.* **2013**, *3*, 3275–3282. [CrossRef] [PubMed]

79.   Loria, S.F.; Prendini, L. Out of India, thrice: Diversification of Asian forest scorpions reveals three colonizations of Southeast Asia. *Sci. Rep.* **2020**, *10*, 22301. [CrossRef] [PubMed]

80.   Bharti, D.K.; Edgecombe, G.D.; Karanth, K.P.; Joshi, J. Spatial patterns of phylogenetic diversity and endemism in the Western Ghats, India: A case study using ancient predatory arthropods. *Ecol. Evol.* **2021**, *11*, 16499–16513. [CrossRef]